Endocrinology

Mutant mice with calcium-sensing receptor (CaSR) activation have hyperglycemia, that is rectified by calcilytic therapy

--Manuscript Draft--

Manuscript Number:	en.2017-00111R1
Full Title:	Mutant mice with calcium-sensing receptor (CaSR) activation have hyperglycemia, that is rectified by calcilytic therapy
Article Type:	Research Article
Section/Category:	Diabetes, Pancreatic and Gastrointestinal Hormones
Corresponding Author:	Rajesh V Thakker, MD ScD FRCP FRCPath FMedSci FRS University of Oxford Headington, Oxford, UNITED KINGDOM
Additional Information:	
Question	**Response**
MANUSCRIPT HISTORY: Has the manuscript been submitted or reviewed before in an Endocrine Society journal?	No
INVITED SUBMISSION: Is this an invited submission?	No
SPECIAL REQUESTS: Enter specific comments or requests to the editors here. Enter “none” if there aren’t any.	None
EDITOR-IN-CHIEF SELECTION: Select an Editor-in-Chief to handle your manuscript: Dr. Andrea Gore or Dr. Stephen Hammes.	Dr. Andrea Gore

WELLCOME TRUST / RESEARCH COUNCILS UK: In accordance with Wellcome Trust and Research Councils UK policies, the Endocrine Society will deposit to PubMed Central the final published article. For the full policy, see the Instructions to Authors. Indicate if the paper you are submitting has received funding from any of the organizations listed below:	Medical Research Council (MRC); Wellcome Trust
STEROID HORMONE MEASUREMENT: I have read and understood the Steroid Hormone Measurement policy and describe my submission as follows:	Not applicable to my manuscript.
CELL LINE AUTHENTICATION: I have read and understood the Cell Line Authentication policy and describe my submission as follows:	My manuscript includes cell lines and meets the standards described in the Cell Line Authentication policy.
PRECIS: Please submit a brief description of your paper that will appear on the Table of Contents along with the title, should your paper be accepted. The description should be NO LONGER THAN 200 CHARACTERS and should serve to buttress the content of the title by simply stating what was done and what was concluded.	Mice with a germline gain-of-function CaSR mutation have hypoinsulinemia, hyperglucagonemia, reduced pancreatic islet mass; and impaired glucose tolerance, which is rectifiable by calcilytic therapy.
Funding Information:	Medical Research Council (G9825289) — May Professor of Medicine Rajesh V Thakker Medical Research Council (G1000467) — May Professor of Medicine Rajesh V Thakker
Requested Editor:	Daniel D Bikle, MD, PhD, Associate Editor
Author Comments:	F.M.H. and R.V.T. have received grant funding from GlaxoSmithKline and NPS/Shire Pharmaceuticals for studies involving the use of calcium-sensing receptor allosteric inhibitors. R.V.T. has also received grants from Novartis Pharma AG and the Marshall Smith Syndrome Foundation for unrelated studies. Duncan Richards is an employee of

	GlaxoSmithKline.

MS ID#: Endocrinology en.2017-00111 Response to Editors' and Reviewers' Comments.

We thank the editors and reviewers for their detailed and supportive comments. We are delighted to learn from the editor's letter that this manuscript "…should be acceptable for publication in Endocrinology pending minor revisions as suggested by the reviewers…" and that "…both reviewers liked this study…" Moreover, we are grateful for the reviewers' supportive comments, and note that: reviewer #1 states that "…These findings are both biologically and clinically significant…"; and reviewer #2 states that "…The studies were methodically and rigorously conducted and the manuscript easy to read and well-written…"

We have addressed the editors' and reviewers' comments, undertaken additional experiments and provided the information that was requested.

en.2017-00111 - Editors' Comments

Raj, both reviewers liked this study. However, each had a number of concerns. Chief among them is the limited number of animals used for a number of the studies, which made it hard to form firm conclusions. I recommend that these numbers be increased. Moreover, the gender differences need to be addressed. I am rating this as a minor revision, but in some cases new data will need to be provided.

We thank the editor for these helpful comments, and over the past 8 weeks we have utilized additional mice for the in vivo glucose tolerance testing, as well for the ex vivo electrophysiological and hormone secretion experiments to ensure that all data has been generated from a minimum of n=4 biological replicates. We have also made clear in the Results section that there were differences in plasma insulin and glucagon concentrations between male and female mice, and also highlighted the differing responses of male and female mice to treatment with the ronacaleret drug compound. Moreover, in response to a comment from reviewer #1 about the effect of glucose on calcium-sensing receptor (CaSR) activation, we have undertaken additional cellular studies to characterize the effect of alterations in glucose concentrations on CaSR signaling responses. This additional data has necessitated the inclusion of Dr Caroline Gorvin as a co-author, and all of the authors are agreed to the inclusion of this individual in the authorship, as well as her position in the authorship order.

en.2017-00111 - Reviewers' Comments

Reviewer #1: Babinsky et al took in vivo and in vitro approaches to investigate the impact of an activating CaSR mutation (Leu723Gln, also named Nuf mutation) on energy metabolism and pancreatic α- and β-cell functions. The animal studies which were well performed showed the development of hypocalcemia, hypoinsulinemia, and impaired glucose tolerance and secretion of insulin and glucagon in +/Nuf or Nuf/Nuf mice carrying, respectively, heterozygous or homozygous germ-line CaSR mutation. These defects were partly rectified by oral administrations of Ronacaleret, an allosteric CaSR antagonist, supporting a role for the CaSR in mediating energy metabolism. These findings are both biologically and clinically significant.

We are grateful to the Reviewer for the supportive comments that the animal studies "…were well performed …" "…supporting a role for the CaSR in mediating energy metabolism…" and that "…These findings are both biologically and clinically significant…"

The authors then cultured pancreatic islets from wt and Nuf/Nuf mice and performed ex vivo insulin and glucagon secretion assays (Figure 6) to elucidate cell-autonomous actions of Wt vs Nuf CaSRs. Their results convincingly showed no significant difference in the ability of raising glucose concentration (from 1 to 6 mM) to induce insulin secretion between two genotypes (Figure 6A,B), but a defect in the glucose-induced suppression of glucagon secretion (Figure 6C,D), supporting a cell-autonomous action of CaSR in α-cells.

We thank the Reviewer for these helpful and supportive comments.

In separate experiments, the authors further tested the effects of changing [Ca2+]o (from 0.8 to 1.6 mM) on the glucose-induced insulin (Figure 6E) and glucagon (Figure 6F) secretion. However, the sample sizes for some data points were small (N =3 or 4) and had large variations, so the results are difficult to interpret for a clear conclusion.

We are grateful to the reviewer about this important point regarding the sample sizes in Figures 6E-F. Over the past 8 weeks, we have undertaken additional studies using cultured pancreatic islets to increase the sample sizes. In particular, we used an additional N=3 Casr$^{Nuf/Nuf}$ mice to increase the batches of Nuf/Nuf islets previously studied from N=3 to N=5-8 batches of islets (highlighted in yellow in figure below), and this increase in the sample size has not affected the significance of our findings. We have amended Figures 6E-F with this additional data (please see below).

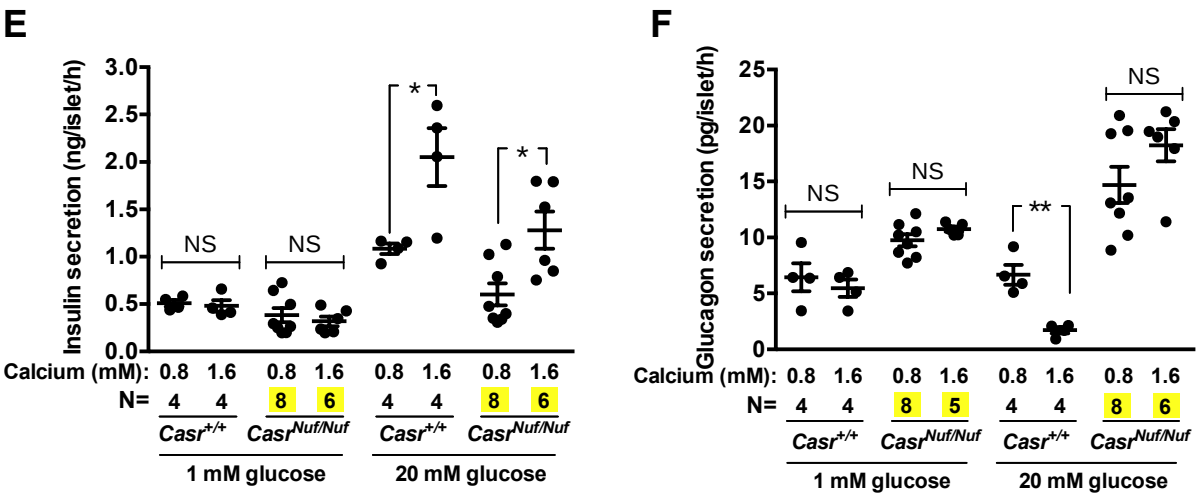

Moreover, we have inserted the following text in the figure 6 legend regarding the sample sizes: "…The sample size (N) represents batches of size-matched islets, which were pooled from 3-6 Casr$^{+/+}$ mice and 6 Casr$^{Nuf/Nuf}$ mice…"

Furthermore, there was no clear rational for choosing 0.8 and 1.6 mM Ca, over the ones in the range (2-5 mM) in which wt and Nuf CaSRs display different signaling capacities (Figure 2). These pitfalls prevent a clear conclusion on a role of CaSR in rendering β-cells ablility to sense and respond to changes in [Ca2+]o.

We thank the reviewer for this comment, and would like to explain that for these ex vivo studies, we used 0.8 mM calcium to simulate the prevailing circulating ionized calcium concentrations in Casr$^{Nuf/Nuf}$ mice, as we have previously reported Casr$^{Nuf/Nuf}$ mice to have albumin-adjusted calcium concentrations of 1.5-1.6 mM, which is equivalent to ionized calcium concentrations of 0.75-0.80 mM (Hough et al PNAS 2004, Hannan et al Endocrinology 2015). We also used 1.6 mM calcium, as this has been reported to represent a physiological calcium concentration, which is used in ex vivo studies involving Krebs-Ringer Buffer solutions (MacConaill J Pharmacol Methods 1985), it coincidentally represents a ~2-fold increase in the prevailing concentrations in Casr$^{Nuf/Nuf}$ mice. To clarify this, we have amended the Results text, as follows: "…size-matched islets were isolated from Casr$^{+/+}$ and Casr$^{Nuf/Nuf}$ mice, and exposed to low (1 mM), physiological (6 mM) or high (20 mM) glucose concentrations in the presence of 1.6 mM $[Ca^{2+}]_o$, which represents a physiological $[Ca^{2+}]_o$ (36)…" and "…To investigate whether the reduced plasma insulin concentrations of Nuf mice may have been a consequence of their hypocalcemia, insulin secretion from isolated islets was measured following exposure to 0.8 mM $[Ca^{2+}]_o$, which is similar to the plasma calcium concentrations observed in Casr$^{Nuf/Nuf}$ mice (15,16)…" Moreover, we have inserted the following text in the Methods: "…A Krebs-Ringer buffer containing 0.8 mM $CaCl_2$ was used to evaluate the effect of lowering the $[Ca^{2+}]_o$ on islet hormone secretion…" and inserted an additional reference regarding the use of physiological (1.6 mM) calcium concentrations in Ringer solutions: "…36. MacConaill M. Calcium precipitation from mammalian physiological salines (Ringer solutions) and the preparation of high [Ca] media. J Pharmacol Methods 1985; 14:147-155…"

The authors compared pancreatic islets sizes and numbers by standard histology (Figure 5A), which convincingly showed fewer and smaller islets in +/Nuf and Nuf/Nuf pancreata.

We thank the Reviewer for this supportive comment.

They further performed immunohistochemistry to quantify α- and β-cell numbers in islets of wt and Nuf mice and concluded that there were modestly reduced β-cell numbers (Figure 5E,F), but increased α-cell (Figure 5E,G) numbers in the Nuf mutant mice. However, the methods used to quantify these cell numbers and normalize the data (Figure 5F,G) were not described

We are grateful to the reviewer for this comment, and have inserted the following text in the Methods to clarify how the cell numbers were quantified and normalized: "…The numbers of α- and β-cells within individual islets were quantified using the cell-based analysis profile of the TissueQuest software (27), and normalized to the total islet area, and reported as percentage of the mean numbers of $Casr^{+/+}$ α- and β-cells, respectively…"

The authors intended to measure cell proliferation rate by Ki-67 staining. However, it's to be reminded that Ki-67 only indicates the status of cell proliferation, but not the speed of proliferation. To assess cell proliferation rates, BrdU incorporation over a given period of time is a better approach.

We agree with the reviewer that Ki-67 staining indicates the status of cell proliferation, but not the proliferation rate, and have amended the y-axis title of the Ki67 graphs (panels I-J in Figure 5), so that this reads as "…% of proliferating…cells…" rather than "…% proliferation rate…". Moreover, we have modified the Results text, as follows: "…The percentage of proliferating insulin-positive β-cells in $Casr^{Nuf/Nuf}$ mice was found to be significantly decreased ($p < 0.05$), whereas the percentage of proliferating insulin-negative cells (which are predominantly α-cells) was significantly increased when compared to respective $Casr^{+/+}$ islets (Figure 5I-J)…" Furthermore, in the Discussion, we have highlighted the advantages of using BrdU incorporation to assess proliferation, as follows: "…β-cell proliferation was measured using the Ki67 marker, which shows proliferation over a limited timeframe, and long-term continuous labeling with the thymidine analog 5-bromo-2-deoxyuridine (BrdU) is required to provide a more accurate assessment of proliferation (43)…" The inclusion of this text in the Discussion has necessitated the insertion of an additional reference: "…43. Walls GV, Reed AA, Jeyabalan J, Javid M, Hill NR, Harding B, Thakker RV. Proliferation rates of multiple endocrine neoplasia type 1 (MEN1)-associated tumors. Endocrinology 2012; 153:5167-5179..."

The authors should also consider the possibility that cell death may contribute to recued islet number and size in the Nuf mice.

We thank the reviewer for this important point, and have modified the Discussion text to emphasize this, as follows: "…alterations in cellular proliferation can substantially impact on adult β-cell mass and insulin secretory capacity (42). Furthermore, the CaSR may have influenced β-cell apoptosis, which has been shown to contribute to the reduced islet mass in humans with type 2 diabetes (44)…" We have also inserted the following reference: "…44. Butler AE, Janson J, Bonner-Weir S, Ritzel R, Rizza RA, Butler PC. Beta-cell deficit and increased beta-cell apoptosis in humans with type 2 diabetes. Diabetes 2003; 52:102-110..."

The authors performed whole-cell recordings to compare electrophysiological activities in α- and β-cells of Wt vs Nuf mice and their responses to different glucose and Ca concentrations. Their data suggest that impaired electrophysiological responses to glucose and tolbutamide (KATP channel blockers) may underlie the aberrant glucagon secretion in α-cells of Nuf mice. Again, the rationale for choosing 0.75 and 1.5 mM Ca in these experiments was not provided.

We are grateful to the reviewer for this comment, and would like to explain that 1.5 mM represents a standard physiological calcium concentration used in previously reported electrophysiological studies involving intact islets (e.g. Shigeto et al. J Clin Invest 2016). We also used 0.75 mM calcium to simulate the circulating ionized calcium concentrations of 0.75-0.80 mM in $Casr^{Nuf/Nuf}$ mice (Hough et al PNAS 2004,

Hannan et al Endocrinology 2015); moreover we choose 0.75 mM rather than 0.80 mM as it represents a 50%, as opposed to 46.7% reduction, and allows measurements following a 2-fold change in calcium, and is consistent with the 2-fold change in the secretion studies of Figures 6E and 6F. We have clarified the use of these calcium concentrations by modifying the Methods text, as follows: "…Islets were immobilised using a wide-bore glass suction pipette (24) and perfused with modified Krebs-Ringer solution (140 mM NaCl, 3.6 mM KCl, 1.5 mM $CaCl_2$, 0.5 mM $MgSO_4$, 10 mM HEPES, 0.5 mM NaH_2PO_4 and $NaHCO_3$ at pH 7.4 with NaOH, and glucose as indicated), as reported (25). A Krebs-Ringer solution containing 0.75 mM $CaCl_2$ was used to evaluate the effect of lowering the $[Ca^{2+}]_o$ on islet electrical activity…" and by inserting the following text in the Results: "…The electrophysiological experiments were undertaken at 1.5 mM $[Ca^{2+}]_o$, as described (25), and the effect of lowering the $[Ca^{2+}]_o$ on β-cell electrical activity was evaluated at 0.75 mM $[Ca^{2+}]_o$, which is in keeping with the plasma calcium concentrations of $Casr^{Nuf/Nuf}$ mice (15,16)…"

In addition, voltage-clamping protocols for the experiments described in Figure 8 were not clearly described.

We apologize to the reviewer for not clearly describing this, and have inserted the following text in the Methods: "…The conductance of the β-cell ATP-sensitive K^+ (K_{ATP}) channel within intact islets was measured using the perforated patch clamping technique following exposure to different glucose concentrations or to tolbutamide (24). During the K_{ATP} channel conductance studies, β-cells were held at -70 mV, and K^+ currents were evoked by exposing the cells to alternating 50 ms pulses of -60 or -80 mV (25)…"

It is also unclear how many mice and batches of islets were used in these electrophysiological studies. Considering their large variations, some data points with N= 3 or 4 seem to be statistically underpowered, delegitimizing the authors' interpretation and conclusion.

We are grateful to the reviewer about this important point, and during the revision of this manuscript we undertook additional electrophysiological experiments to increase the sample sizes. We have updated figures 7 and 8 with this additional data (please see updated figures on pages 11 & 12 of this response letter), and the increase in the sample sizes has not affected the significance of our findings. Moreover, we have inserted the following text in the legends to figures 7-9 to clarify what the sample sizes represent:

Figure 7 legend: "…The sample size (N) represents individual β-cell recordings obtained from intact islets of 6 $Casr^{+/+}$ mice and 4 $Casr^{Nuf/Nuf}$ mice…"

Figure 8 legend: "…The sample size (N) represents individual β-cell recordings obtained from intact islets of 5 $Casr^{+/+}$ mice and 5 $Casr^{Nuf/Nuf}$ mice…"

Figure 9 legend: "…The sample size (N) represents individual α-cell recordings obtained from intact islets of 5 $Casr^{+/+}$ mice and 7 $Casr^{Nuf/Nuf}$ mice…"

Other comments:
Materials and Methods:

- Page 8, 2nd paragraph: In islet insulin and glucagon secretion assays, the [Ca] bathing the islets before they were switched to 0.8 and 1.6 mM Ca was not stated.

We thank the Reviewer for this comment and to clarify the calcium concentration that the islets were incubated in, we have modified the Methods text, as follows: "…Batches of 13 size-matched islets were incubated for 1 hour at 37°C in 0.3 ml of modified Krebs-Ringer buffer containing 2mg/ml BSA, 1.6 mM $CaCl_2$ and 3mM glucose, followed by a 1 hour incubation in 0.3 ml of the same Krebs-Ringer buffer supplemented with 1, 6 or 20 mM glucose, as described (21)…"

- Sample sizes in some data points in Figures 3, 4, 6, and 8 and supplementary Figure 3 are too small and statistically underpowered.

We are grateful to the reviewer for this comment, and over the past 8 weeks we have utilized additional mice for the in vivo glucose tolerance testing, as well for the ex vivo electrophysiological and hormone secretion experiments to ensure that all data has been generated from a minimum of n=4 biological replicates. We have incorporated this additional data into Figures 3, 4, 6, 7 and 8; and also into supplementary Figure 1 and supplementary Figure 3 (which is now relabelled as supplementary Figure 4). Increasing the sample sizes has not altered the significance of our findings (please see updated figures on pages 8-14 of this response letter).

Results:

- Figure 2B and 2C: Have the authors tested whether glucose allosterically modulates CaSR activation in their assays as previously reported (www.jbc.org/content/291/44/23126) and whether Nuf mutant has different responses to glucose.

We thank the reviewer, and to address this important comment we have generated HEK293 cells stably expressing the WT and mutant Nuf CaSRs, and evaluated whether glucose may allosterically modulate CaSR function in these cells. Our studies have demonstrated that varying the extracellular glucose from 3 mM to 25 mM had no significant effect on the intracellular calcium signaling responses of cells expressing WT or mutant Nuf CaSRs.

We have inserted this data as Supplementary Figure 3 (please see page 6 of the response letter), and also inserted the following text in the Results: "…Glucose has recently been reported to lead to allosteric activation of the CaSR (30), and we investigated the effect of alterations in glucose concentrations on the $Ca^{2+}{}_i$ responses of WT and Nuf mutant Gln723 CaSRs, which were stably expressed in HEK293 cells (Supplemental Figure 3). Our findings showed that altering the glucose concentration from 3 mM to 25 mM had no effect on the EC_{50} values of cells stably expressing WT or Nuf mutant Gln723 CaSRs, whereas the addition of 40 nM ronacaleret significantly increased the EC_{50} values of these cells (Supplemental Figure 3)…"

Moreover, we have inserted the following text in the Discussion: "…Although our studies showed CaSR activation to influence plasma glucose concentrations, we did not observe any effect of extracellular glucose on the acute signalling responses of WT or mutant Nuf CaSRs in vitro. Our findings are consistent with results obtained by other groups (personal communications from A. Conigrave and D. Ward), but contrast with a recent study, which showed that raising the glucose concentration from 3 to 5 mM increased the $Ca^{2+}{}_i$ responses of stably expressing HEK293-CaSR cells in the presence of $Ca^{2+}{}_o$ (30). This recent study, which showed glucose to act as a CaSR allosteric activator, measured $Ca^{2+}{}_i$ responses in single cells using the fluo-8 calcium binding dye (30), whereas, our study measured $Ca^{2+}{}_i$ responses in populations of HEK293-CaSR cells using the fluo-4 calcium binding dye; and these methodological differences may be contributors to the contrasting observations of these two studies…"

We have also inserted the following reference: "…30. Medina J, Nakagawa Y, Nagasawa M, Fernandez A, Sakaguchi K, Kitaguchi T, Kojima I. Positive Allosteric Modulation of the Calcium-sensing Receptor by Physiological Concentrations of Glucose. J Biol Chem 2016; 291:23126-23135…"

Furthermore, we have inserted the following Methods text and references in the Supplementary section:

"…Supplemental Methods: Assays to assess glucose as an allosteric modulator were performed in HEK293 cells that stably expressed either the WT or mutant Gln723 CaSR proteins. These cells were generated using HEK293 T-Rex-Flp-in stable cell-lines (Life Technologies), as reported (1). $Ca^{2+}{}_o$-induced $Ca^{2+}{}_i$ responses were measured using Fluo-4 Ca^{2+} assays adapted from methods previously published (2). Cells were plated in poly-L-lysine treated black-walled 96-well plates (Corning), and 12 hours later incubated in media containing 1µg/ml tetracycline (Invitrogen) to induce CaSR protein expression. On the following day, cells were incubated for 30 min in an extracellular solution composed of 140 mM NaCl, 5 mM KCl, 1 mM $MgCl_2$, 1.3 mM $CaCl_2$ and 10 mM HEPES (pH7.3), and either 3 mM, 5 mM, or 25 mM glucose (all obtained from Sigma) (3). Solutions were normalized for osmolarity (by adjusting NaCl concentrations) and pH. For studies involving ronacaleret, cells were incubated in an extracellular solution containing 3 mM glucose and 40 nM ronacaleret at 37°C. Cells were then loaded with the Fluo-4 Ca^{2+}-binding dye, which was prepared according to manufacturer's instructions (Invitrogen) and incubated for a further 30 min at 37°C (2). The $Ca^{2+}{}_i$ assays were performed on a PHERAstar instrument (BMG Labtech) at 37°C with an excitation filter of 485nm and an emission filter of 520nm. Baseline measurements were made and increasing doses of $CaCl_2$ (0-15 mM)

injected automatically into each well. The peak mean fluorescence ratio of the transient response after each individual stimulus was measured using MARS data analysis software (BMG Labtech), and expressed as a normalized response. Nonlinear regression of concentration-response curves was performed with GraphPad Prism using the normalized response at each $[Ca^{2+}]_e$ for each separate experiment for the determination of the EC_{50} (i.e. $[Ca^{2+}]_e$ required for 50% of the maximal response). Assays were performed in 8 biological replicates for each of the expression constructs. Statistical analysis was performed using the F-test (4).

Supplemental references:

1. Babinsky VN et al. Allosteric Modulation of the Calcium-sensing Receptor Rectifies Signaling Abnormalities Associated with G-protein alpha-11 Mutations Causing Hypercalcemic and Hypocalcemic Disorders. The Journal of biological chemistry. 2016;291(20):10876-85.

2. Leach K et al. Towards a structural understanding of allosteric drugs at the human calcium-sensing receptor. Cell research. 2016;26(5):574-92.

3. Medina J et al. Positive Allosteric Modulation of the Calcium-sensing Receptor by Physiological Concentrations of Glucose. The Journal of biological chemistry. 2016;291(44):23126-35.

4. Gorvin CM et al. Galpha11 mutation in mice causes hypocalcemia rectifiable by calcilytic therapy. JCI insight. 2017;2(3):e91103…."

Supplementary Figure 3:

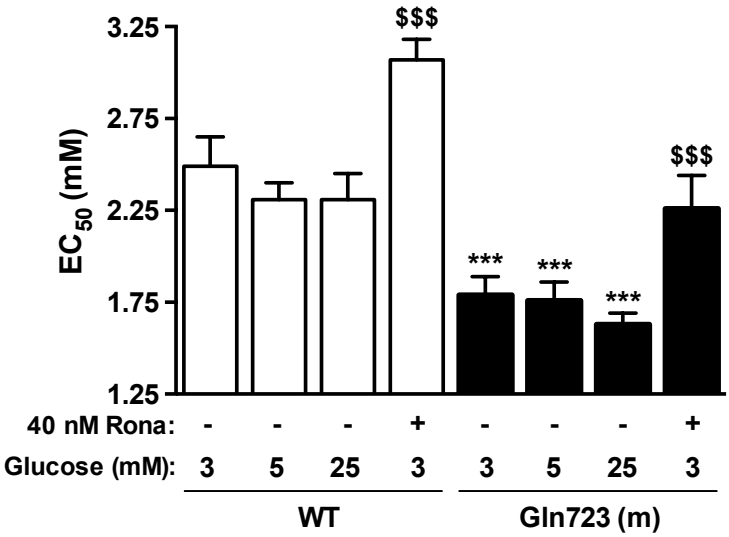

*Supplementary Figure 3. Effect of glucose on the intracellular calcium EC_{50} values of the WT and Gln723 (Nuf) mutant CaSRs. HEK293 cells stably expressing the Gln723 mutant CaSR (black bars) showed significantly reduced EC_{50} values compared to HEK293 cells stably expressing WT CaSR (open bars, ***p<0.001), consistent with a gain-of-function, as previously reported (15,16). Increases in concentrations of glucose from 3-25 mM had no effect on the EC_{50} responses of WT or Gln723 mutant CaSR expressing cells. However, both WT and Gln723 mutant CaSR expressing cells responded to treatment with 40 nM ronacaleret (Rona) and showed significantly increased EC_{50} values compared to respective untreated cells ($^{\$\$\$}p<0.001$). Data is shown as mean ± 95% confidence intervals of 8 independent transfections. These results indicate that glucose is not an allosteric activator of the CaSR.*

[Ca] bathing islets in experiments shown in Figures 6B, 6D, 8, and 9 were not specified.

We are grateful to the reviewer for this comment, and to clarify the calcium concentrations the islets were incubated in, we have modified the text in the legends to figures 6-9, as follows:

Figure 6B legend: "…$Casr^{+/+}$ and $Casr^{Nuf/Nuf}$ islets were incubated in 1.6 mM $[Ca^{2+}]_o$ and exposed to varying glucose concentrations (1 mM, 6 mM or 20 mM)…"

Figure 6D legend: "…$Casr^{+/+}$ and $Casr^{Nuf/Nuf}$ islets were incubated in 1.6 mM $[Ca^{2+}]_o$ and exposed to 1 mM and 6 mM glucose concentrations…"

Figure 7 legend: "…Representative membrane potential recording of β-cells from intact $Casr^{+/+}$ and $Casr^{Nuf/Nuf}$ after islets had been incubated in 1.5 mM $[Ca^{2+}]_o$…"
Figure 8 legend: "…Representative recording of β-cell K_{ATP} channel conductance from intact $Casr^{+/+}$ and $Casr^{Nuf/Nuf}$ islets after islets had been incubated in 1.5 mM $[Ca^{2+}]_o$…"
Figure 9 legend: "…Representative membrane potential recording of α-cells from (A) intact $Casr^{+/+}$ and (B) $Casr^{Nuf/Nuf}$ islets after islets had been incubated in 1.5 mM $[Ca^{2+}]_o$…"

Figure 8A and 8C can be combined, so can Figures 8B and 8D.

We thank the reviewer for this helpful comment, and have combined these panels in Figure 8 (please see amended figure on page 12 of the response letter).

Please verify statistics for the data in Supplementary Figure 4. Some gene expression (e.g., Ccnd2, Foxm1, and Foxo1) appears to be different between wt and Nuf islets.

We are grateful to the reviewer for this comment, and would like to verify that we used the Kruskal-Wallis test for multiple comparisons when analysing this data. No significant differences were observed between $Casr^{+/+}$ and $Casr^{Nuf/Nuf}$ islets, and we have inserted the following the text in the legend to Supplementary figure 4 (now relabelled as Supplementary figure 5): "…Alterations in gene expression between $Casr^{Nuf/Nuf}$ and $Casr^{+/+}$ islets were assessed using the Kruskal-Wallis test for multiple comparisons…"

Figures with amended sample sizes are shown on pages 8-14. The sample numbers that have been increased from n=3-13 to n=5-14 biological replicates are highlighted in yellow.

Figure 3

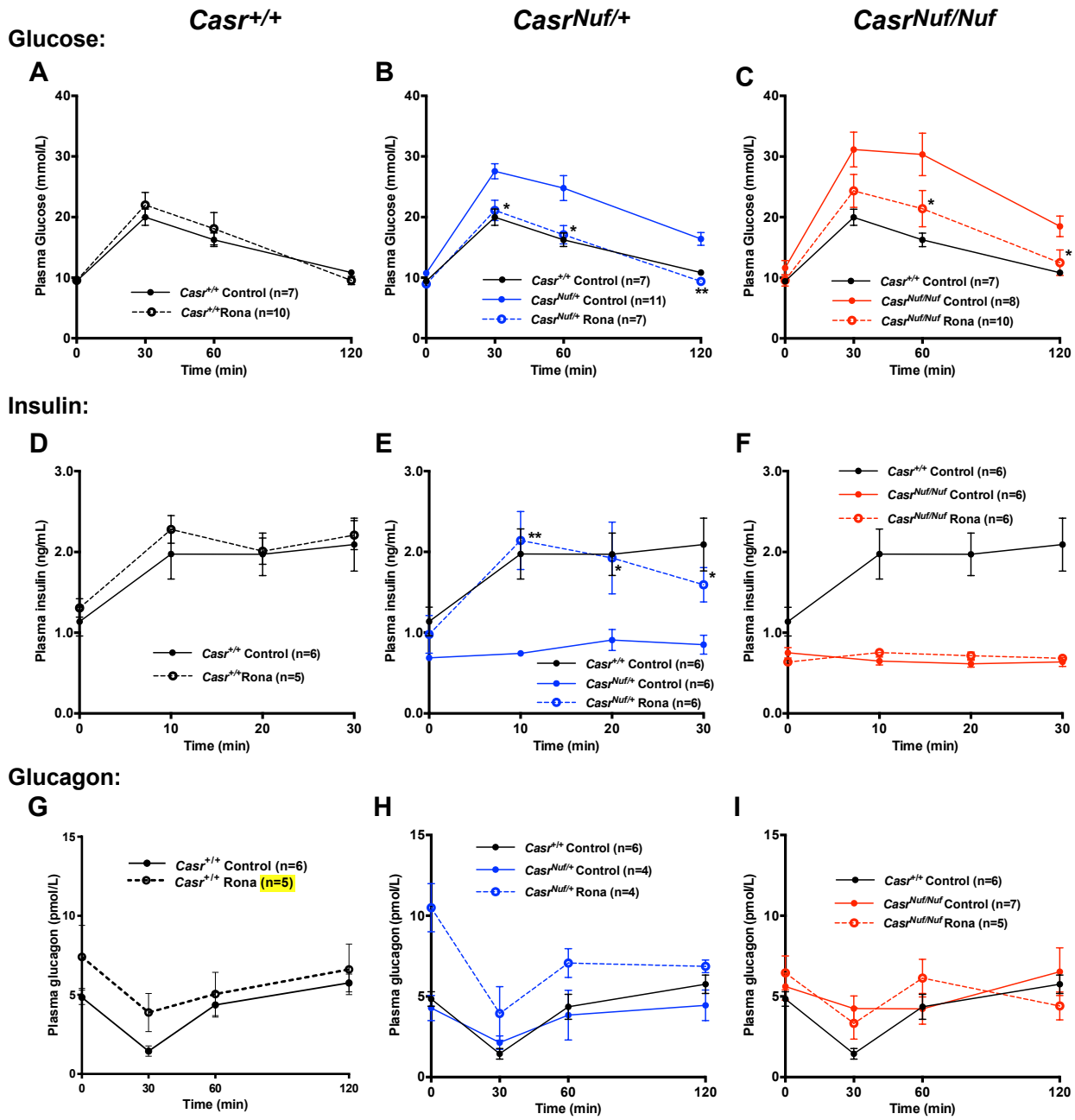
Casr+/+
CasrNuf/+
CasrNuf/Nuf
Glucose:
A
B
C
Plasma Glucose (mmol/L)
Time (min)
Casr+/+ Control (n=7)
Casr+/+Rona (n=10)
CasrNuf/+ Control (n=11)
CasrNuf/+ Rona (n=7)
CasrNuf/Nuf Control (n=8)
CasrNuf/Nuf Rona (n=10)
Insulin:
D
E
F
Plasma insulin (ng/mL)
Casr+/+ Control (n=6)
Casr+/+Rona (n=5)
CasrNuf/+ Control (n=6)
CasrNuf/+ Rona (n=6)
CasrNuf/Nuf Control (n=6)
CasrNuf/Nuf Rona (n=6)
Glucagon:
G
H
I
Plasma glucagon (pmol/L)
Casr+/+ Control (n=6)
Casr+/+ Rona (n=5)
CasrNuf/+ Control (n=4)
CasrNuf/+ Rona (n=4)
CasrNuf/Nuf Control (n=7)
CasrNuf/Nuf Rona (n=5)

Figure 4

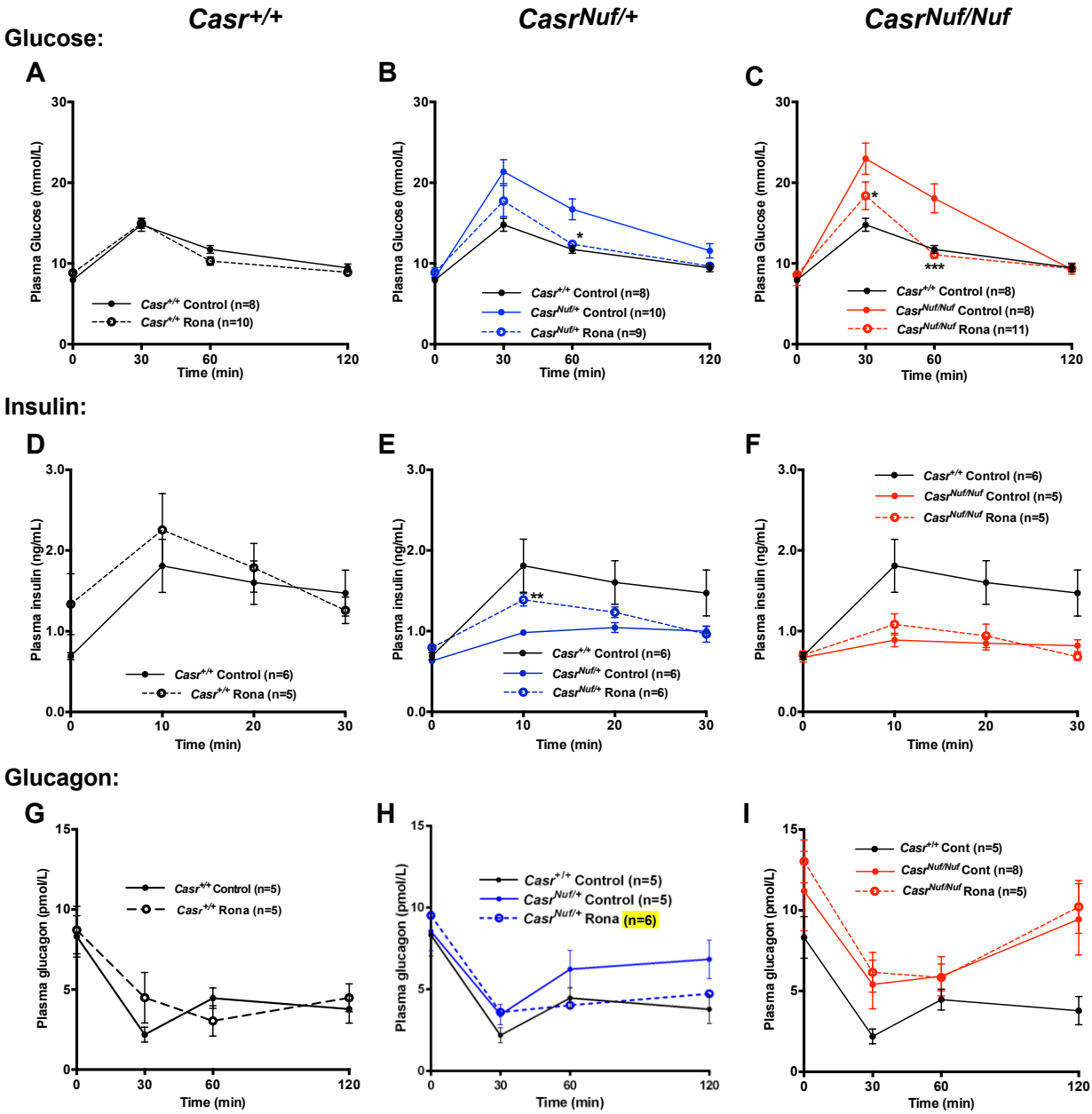
Casr+/+
CasrNuf/+
CasrNuf/Nuf
Glucose:
A
B
C
Plasma Glucose (mmol/L)
Time (min)
Casr+/+ Control (n=8)
Casr+/+ Rona (n=10)
CasrNuf/+ Control (n=8)
CasrNuf/+ Control (n=10)
CasrNuf/+ Rona (n=9)
CasrNuf/Nuf Control (n=8)
CasrNuf/Nuf Rona (n=11)
Insulin:
D
E
F
Plasma insulin (ng/mL)
Casr+/+ Control (n=6)
Casr+/+ Rona (n=5)
CasrNuf/+ Control (n=6)
CasrNuf/+ Rona (n=6)
CasrNuf/Nuf Control (n=5)
CasrNuf/Nuf Rona (n=5)
Glucagon:
G
H
I
Plasma glucagon (pmol/L)
Casr+/+ Control (n=5)
Casr+/+ Rona (n=5)
CasrNuf/+ Control (n=5)
CasrNuf/+ Rona (n=6)
CasrNuf/Nuf Cont (n=8)
CasrNuf/Nuf Rona (n=5)

Figure 6

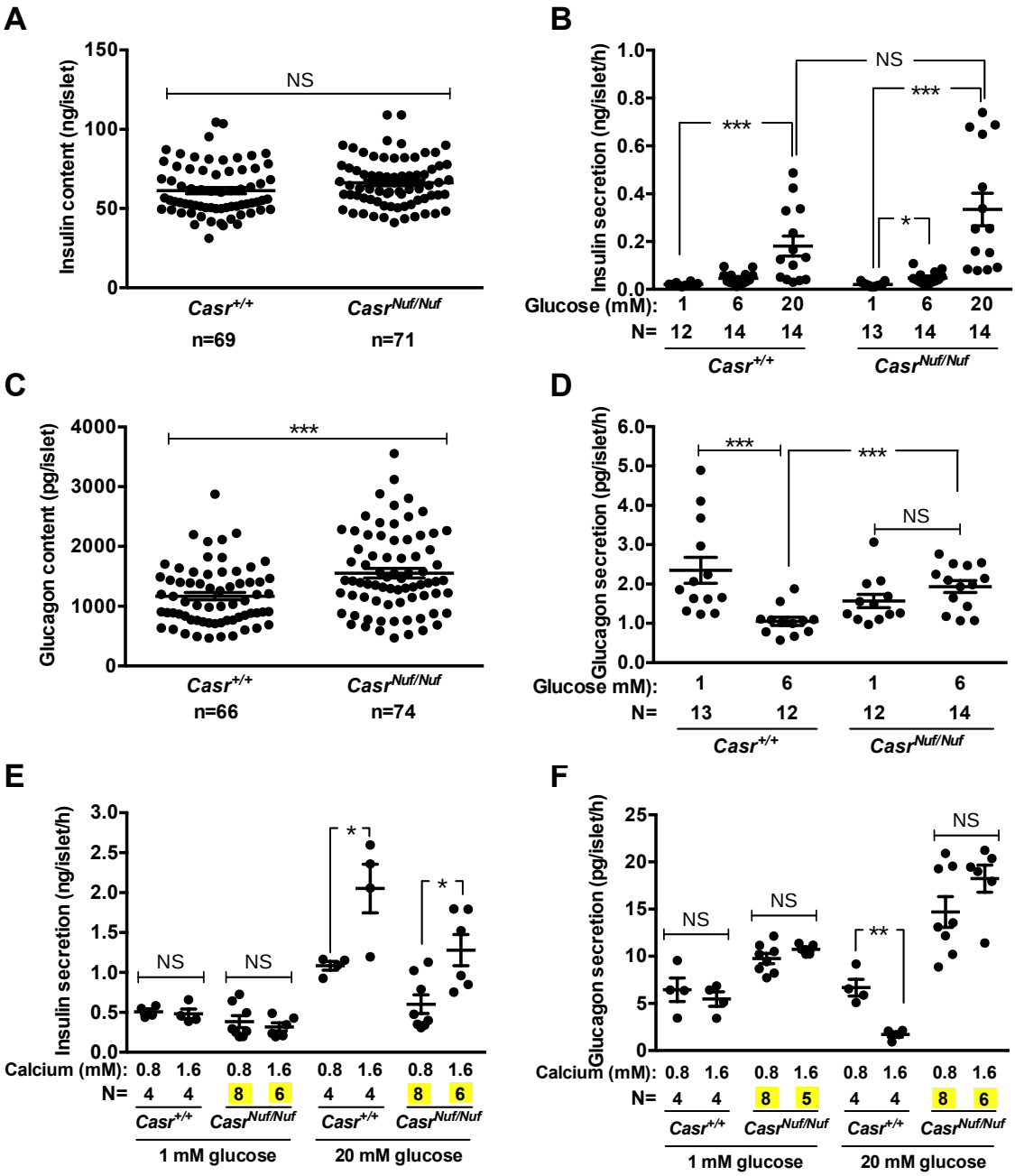
A
Insulin content (ng/islet)
150
100
50
0
NS
Casr+/+
Casr Nuf/Nuf
n=69
n=71
B
Insulin secretion (ng/islet/h)
1.0
0.8
0.6
0.4
0.2
0.0
NS
***
***
*
Glucose (mM): 1 6 20 1 6 20
N= 12 14 14 13 14 14
Casr+/+
Casr Nuf/Nuf
C
Glucagon content (pg/islet)
4000
3000
2000
1000
0
***
Casr+/+
Casr Nuf/Nuf
n=66
n=74
D
Glucagon secretion (pg/islet/h)
6.0
5.0
4.0
3.0
2.0
1.0
0.0
***
***
NS
Glucose mM): 1 6 1 6
N= 13 12 12 14
Casr+/+
Casr Nuf/Nuf
E
Insulin secretion (ng/islet/h)
3.0
2.5
2.0
1.5
1.0
0.5
0.0
NS
NS
*
*
Calcium (mM): 0.8 1.6 0.8 1.6 0.8 1.6 0.8 1.6
N= 4 4 8 6 4 4 8 6
Casr+/+
Casr Nuf/Nuf
Casr+/+
Casr Nuf/Nuf
1 mM glucose
20 mM glucose
F
Glucagon secretion (pg/islet/h)
25
20
15
10
5
0
NS
NS
**
NS
Calcium (mM): 0.8 1.6 0.8 1.6 0.8 1.6 0.8 1.6
N= 4 4 8 5 4 4 8 6
Casr+/+
Casr Nuf/Nuf
Casr+/+
Casr Nuf/Nuf
1 mM glucose
20 mM glucose

Figure 7

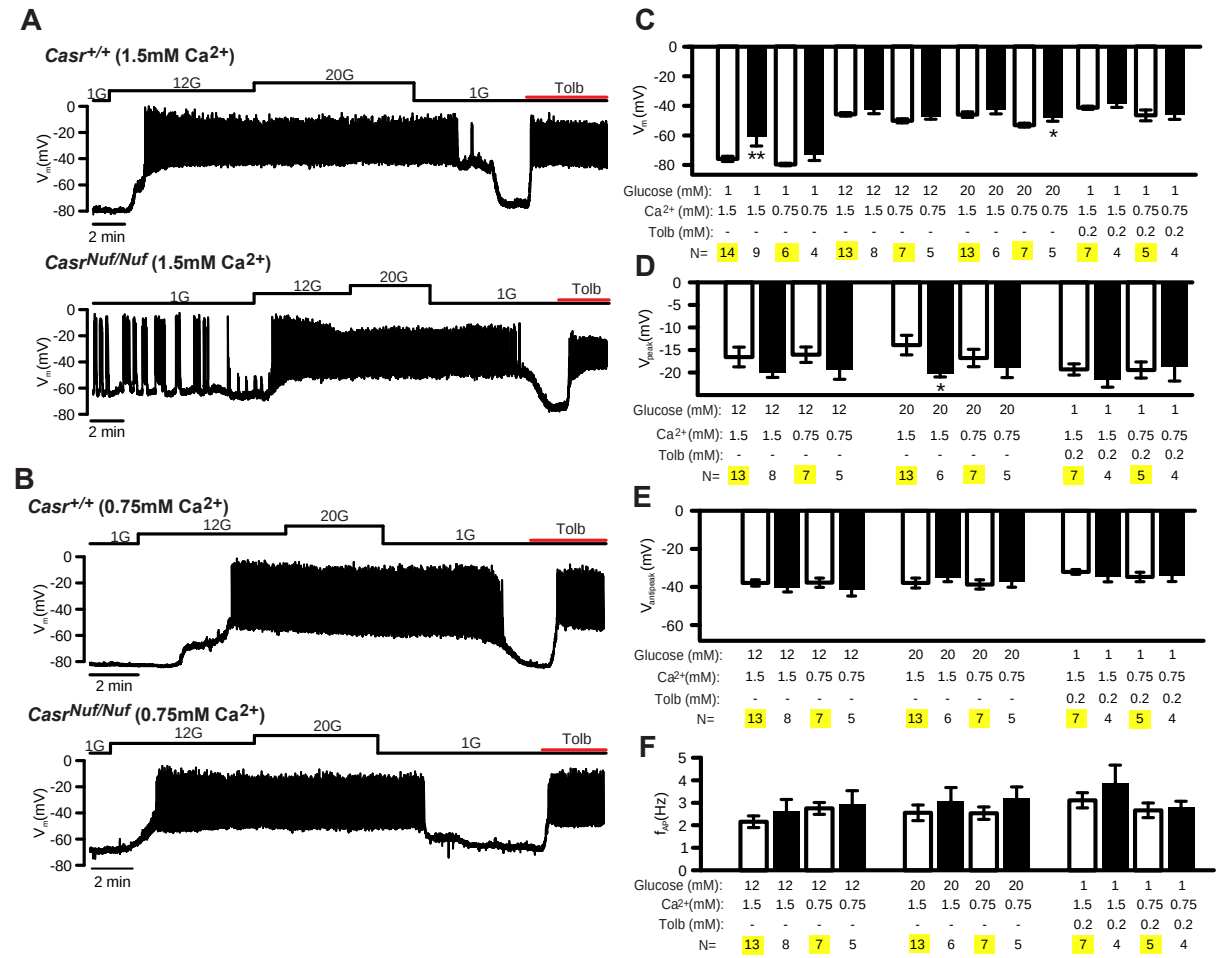
A
Casr+/+ (1.5mM Ca2+)
1G
12G
20G
1G
Tolb
Vm (mV)
2 min
CasrNuf/Nuf (1.5mM Ca2+)
B
Casr+/+ (0.75mM Ca2+)
CasrNuf/Nuf (0.75mM Ca2+)
C
Vm (mV)
Glucose (mM): 1 1 1 1 12 12 12 12 20 20 20 20 1 1 1 1
Ca2+ (mM): 1.5 1.5 0.75 0.75 1.5 1.5 0.75 0.75 1.5 1.5 0.75 0.75 1.5 1.5 0.75 0.75
Tolb (mM): - - - - - - - - - - - - 0.2 0.2 0.2 0.2
N= 14 9 6 4 13 8 7 5 13 6 7 5 7 4 5 4
D
Vpeak (mV)
Glucose (mM): 12 12 12 12 20 20 20 20 1 1 1 1
Ca2+(mM): 1.5 1.5 0.75 0.75 1.5 1.5 0.75 0.75 1.5 1.5 0.75 0.75
Tolb (mM): - - - - - - - - 0.2 0.2 0.2 0.2
N= 13 8 7 5 13 6 7 5 7 4 5 4
E
Vantipeak (mV)
Glucose (mM): 12 12 12 12 20 20 20 20 1 1 1 1
Ca2+(mM): 1.5 1.5 0.75 0.75 1.5 1.5 0.75 0.75 1.5 1.5 0.75 0.75
Tolb (mM): - - - - - - - - 0.2 0.2 0.2 0.2
N= 13 8 7 5 13 6 7 5 7 4 5 4
F
fAP (Hz)
Glucose (mM): 12 12 12 12 20 20 20 20 1 1 1 1
Ca2+(mM): 1.5 1.5 0.75 0.75 1.5 1.5 0.75 0.75 1.5 1.5 0.75 0.75
Tolb (mM): - - - - - - - - 0.2 0.2 0.2 0.2
N= 13 8 7 5 13 6 7 5 7 4 5 4

Figure 8

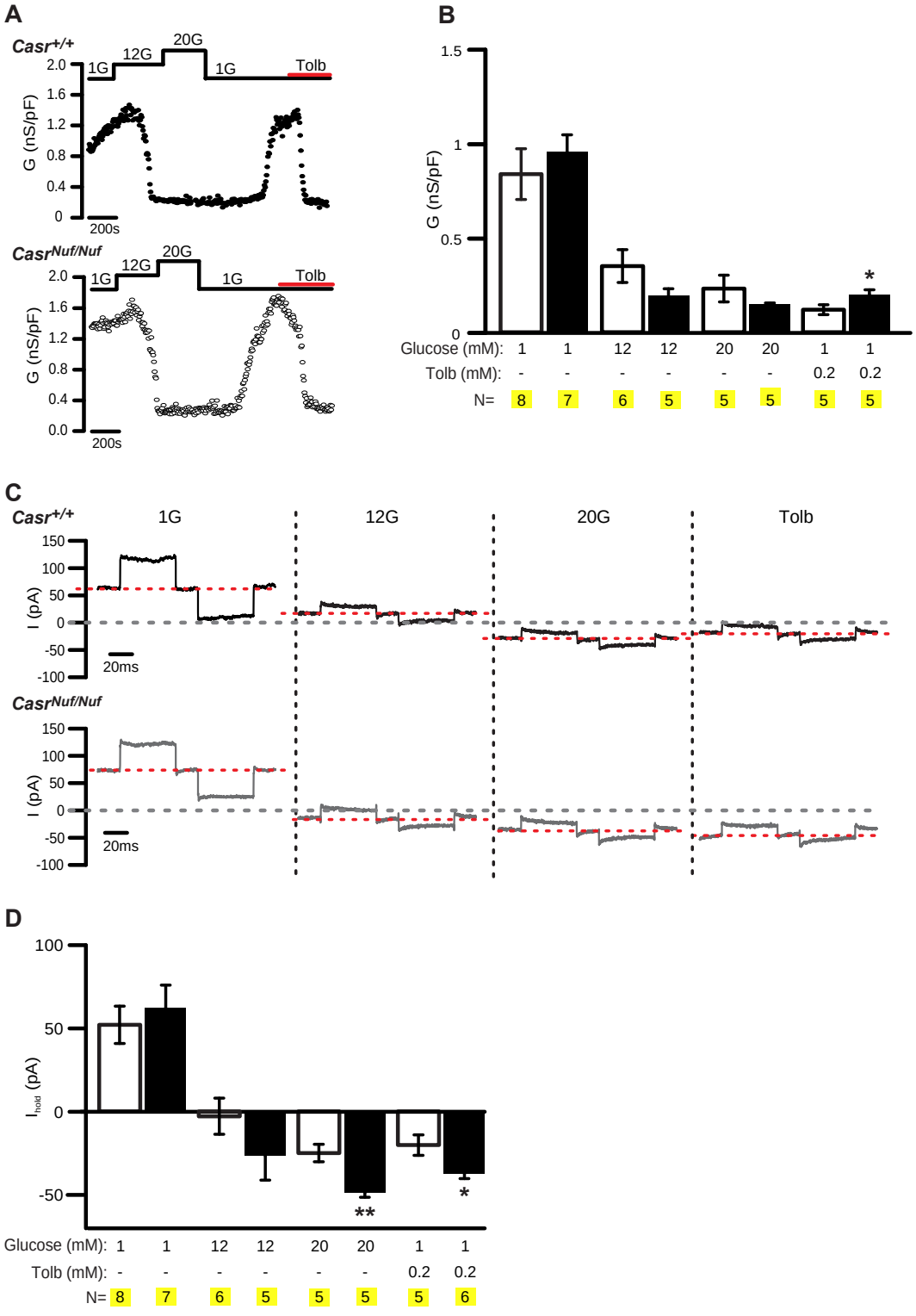
A
Casr+/+
1G
12G
20G
1G
Tolb
G (nS/pF)
200s
CasrNuf/Nuf
B
G (nS/pF)
Glucose (mM): 1 1 12 12 20 20 1 1
Tolb (mM): - - - - - - 0.2 0.2
N= 8 7 6 5 5 5 5 5
C
Casr+/+
1G
12G
20G
Tolb
I (pA)
20ms
CasrNuf/Nuf
D
Ihold (pA)
Glucose (mM): 1 1 12 12 20 20 1 1
Tolb (mM): - - - - - - 0.2 0.2
N= 8 7 6 5 5 5 5 6

Supplementary Figure 1

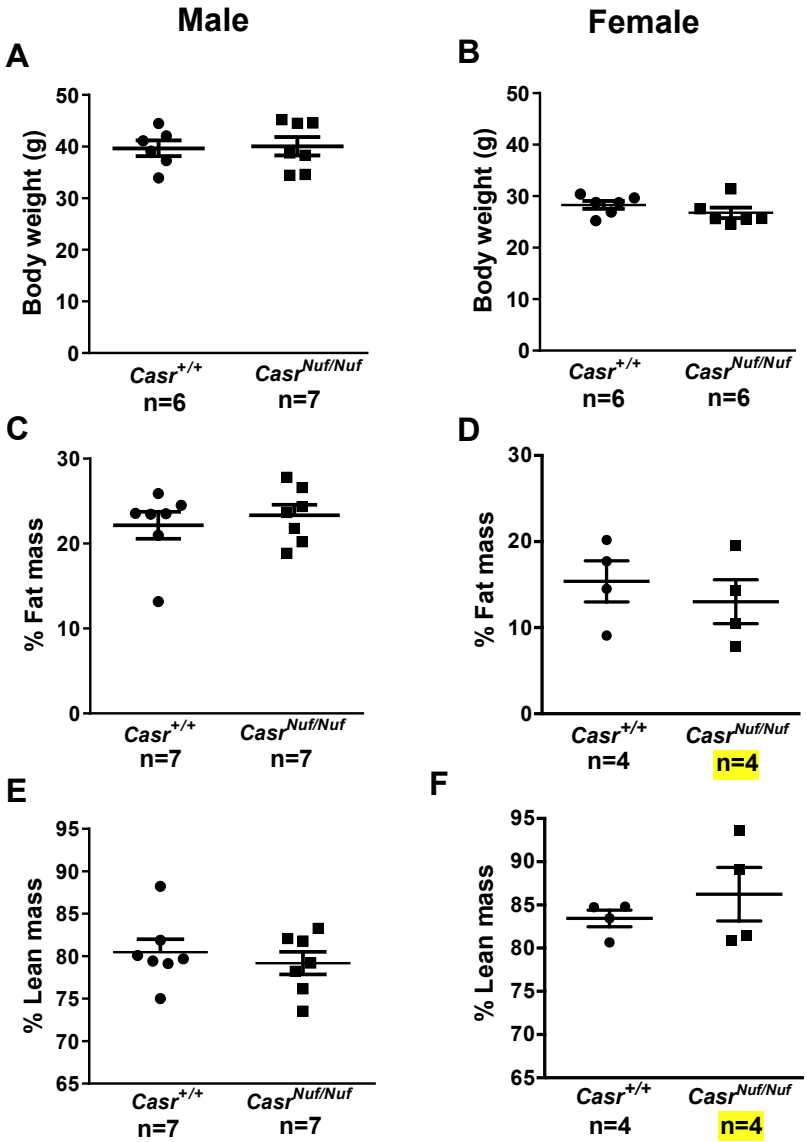

Supplementary Figure 1. Body weight and comp osition of *Nuf* mice. (A-B) Body weight of male and female *Casr*$^{+/+}$ and *Casr*$^{Nuf/Nuf}$ mice. (C-D) Percentage fat mass of male and female *Casr*$^{+/+}$ and *Casr*$^{Nuf/Nuf}$ mice. (E-F) Percentage lean mass of male and female *Casr*$^{+/+}$ and *Casr*$^{Nuf/Nuf}$ mice. Results are expressed as mean ± SEM.

Supplementary Figure 4

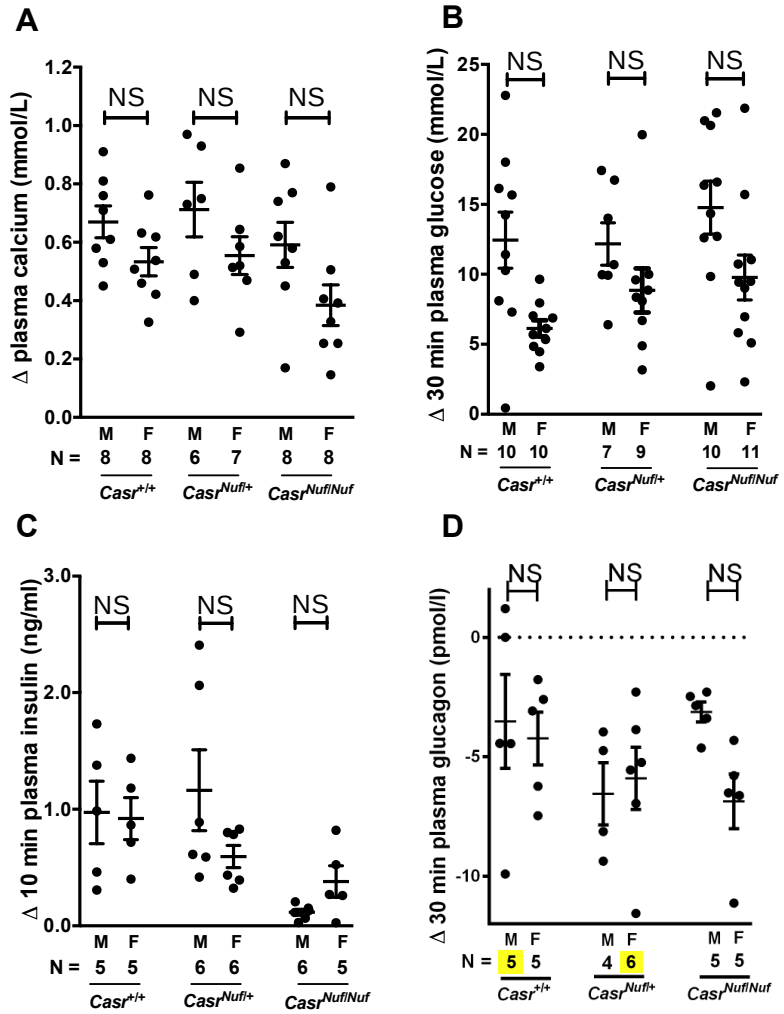

Supplementary Figure 4. Comparison of bioch emical responses of ronacaleret-treated male and female mice. (A) Maximal changes in plasma adjusted-cal cium concentrations of ronacalceret-treated male and female *Casr*$^{+/+}$, *Casr*$^{Nuf/+}$ and *Casr*$^{Nuf/Nuf}$ mice. Maximal changes in plasma concentrations of (B) glucose, (C) insulin and (D) glucagon of ronacalcer et-treated male and female *Casr*$^{+/+}$, *Casr*$^{Nuf/+}$ and *Casr*$^{Nuf/Nuf}$ mice during IPGTT. Mean ± SEM values are represented by solid bars. NS, non-significant.

Reviewer #2: General Statement:
This is a study that evaluated the role of the calcium-sensing receptor (CaSR) in glucose homeostasis in a Casrnuf/+ and Casrnuf/nuf mice, an animal model of autosomal dominant hypocalcemia. The study also looked at the effects of a CaSR antagonist compound, a calcilytic, on glucose homeostasis. The authors found that the Casrnuf/+ and Casrnuf/nuf mice, which have either one or two germline gain-of-function mutations in the CaSR, respectively, had impaired glucose tolerance and insulin secretion. Treatment with the calcilytic improved glucose intolerance. Mutant mice had decreased pancreatic islet mass and β-cell proliferation. There was also evidence for impaired glucagon suppression in response to glucose as well as increased pancreatic α-cells. The studies were methodically and rigorously conducted and the manuscript easy to read and well-written. While there is little evidence that these findings translate to humans with activating mutations in the CaSR, it suggests that the CaSR may play a role in glucose homeostasis in mammals.

We thank the Reviewer for the supportive comments that "…The studies were methodically and rigorously conducted and the manuscript easy to read and well-written…" and "…suggests that the CaSR may play a role in glucose homeostasis in mammals…"
Results:
There was a tendency to overstate some of the results:
1. On page 11, lines 14-16, please clarify the results of the change in insulin concentrations following glucose bolus. Only male Casrnuf/+ mice had statistically different insulin levels than the Casr+/+ mice.

We thank the Reviewer, and have clarified the change in insulin concentrations in male and female mice by modifying the Results text, as follows: "…Plasma insulin concentrations of male and female $Casr^{+/+}$ mice increased two-fold at 10 min after an IP 2g/kg glucose bolus injection (Figure 1C-D). However, male affected $Casr^{Nuf/+}$ and $Casr^{Nuf/Nuf}$ mice showed significantly reduced plasma insulin concentrations at 10 and 20 min following glucose administration (Figure 1C); whereas only female $Casr^{Nuf/Nuf}$ mice showed significantly reduced insulin concentrations at 20 min (Figure 1D), compared to respective $Casr^{+/+}$ mice…"

2. On page 11, lines 16-18, it appears that the female Casrnuf/nuf mice only had one insulin level that was statistically different from the Casr+/+ mice. Please temper wording of "Casrnuf/nuf had no significant insulin response" and the following sentence, "Thus, plasma insulin concentrations were significantly reduced in Nuf mice compared to Casr+/+".

We are grateful to the reviewer for these helpful comments, and have omitted "Casrnuf/nuf had no significant insulin response" from the Results text. Moreover, we have specified which Nuf mice had reduced insulin concentrations by inserting the following text in the Results: "…male affected $Casr^{Nuf/+}$ and $Casr^{Nuf/Nuf}$ mice showed significantly reduced plasma insulin concentrations at 10 and 20 min following glucose administration (Figure 1C); whereas only female $Casr^{Nuf/Nuf}$ mice showed significantly reduced insulin concentrations at 20 min (Figure 1D), compared to respective $Casr^{+/+}$ mice…"

3. On page 11, lines 18-20, please note that the glucagon response was only statistically different at one time point, and clarify the difference between males and females.

We thank the Reviewer, and to address this comment have modified the Results text, as follows: "…Affected male $Casr^{Nuf/Nuf}$ mice were also shown to have an inadequate suppression of plasma glucagon concentrations at the 30 min time-point during a 120 min IPGTT (Figure 1E), whereas female $Casr^{Nuf/Nuf}$ mice had significantly raised plasma glucagon concentrations at 120 min (Figure 1F)…"

4. On page 12, lines 18-20, please note the gender differences in the effect of ronacaleret treatment on glucose tolerance in Casrnuf/+ mice.

We thank the Reviewer, and have inserted the following text in the Results: "…Moreover, gender differences were noted, as ronacaleret normalised plasma glucose concentrations at 30 min in male $Casr^{Nuf/+}$mice, but only at 60 min in female $Casr^{Nuf/+}$mice (Figures 3 and 4)…"

Discussion:

1. In the first paragraph on page 17, lines 3-12, please add that there is no obvious glucose homeostasis phenotype in the patients with ADH-causing mutations (i.e., patients in the literature are not reported to have diabetes) and further, more detailed investigation of glucose homeostasis in humans is warranted.

We are grateful to the reviewer for this comment, and have inserted the following text in the Discussion: "…However, impaired glucose tolerance or diabetes has not been reported in ADH patients to-date, and detailed investigations of glucose homeostasis in humans are warranted…"

2. On page 20, lines 3-5, it seems that one of the "Casrnuf/nuf" should be "Casr+/+" α-cells. Please clarify.

We are grateful to the reviewer for detecting this error and have amended this to "…Casr$^{+/+}$ α-cells…"

Figure 2:

1. In Figure 2B, please change the lines so that they are different colors. Given the overlap of the dashed lines and circular symbols, it is difficult to differentiate between the various lines in both the full graph as well as the zoomed-in image.

We thank the Reviewer, and have amended figure 2B, so that the lines are all different colours (please see below).

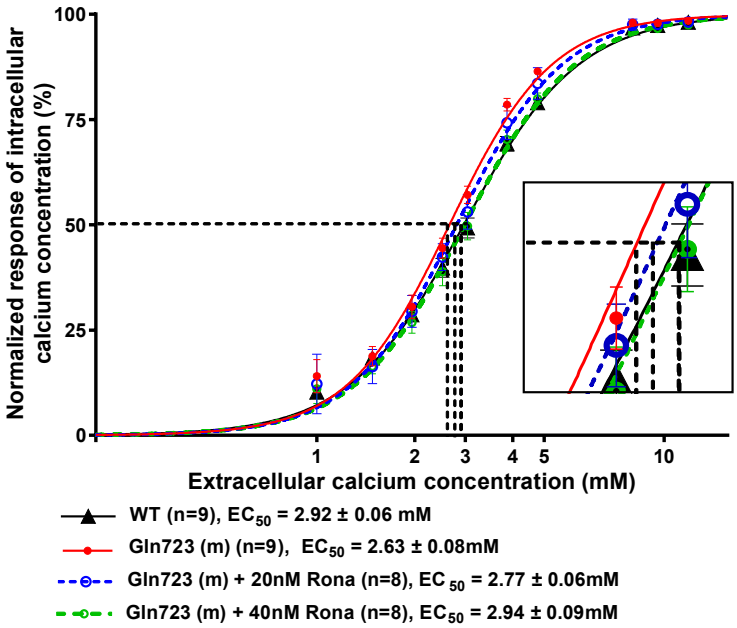

Figure 6:

1. In panel D, there appears to be an extra number included for the "N" in both groups of mice. Please clarify what the middle "N" number between the glucose 1mM and 6 mM is representing.

We are grateful to the reviewer for detecting this error, and have deleted the additional "N" number from figure 6D (please see below).

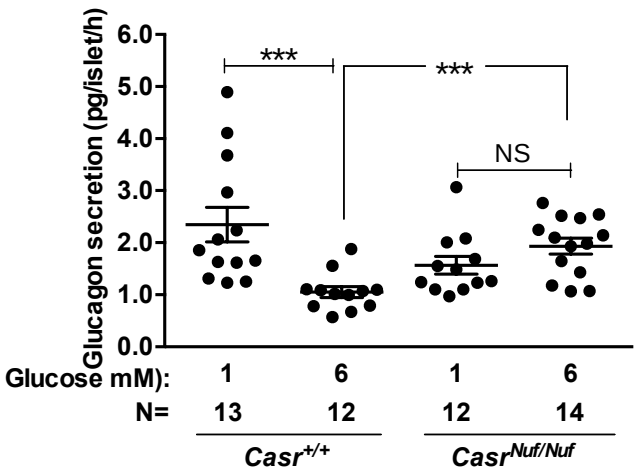

Figure 7:

1. In the legend on page 27, lines 14-15, please clarify whether or not p-values are compared to Casr+/+ mice at respective glucose concentrations alone or respective glucose and calcium concentrations.

*We thank the reviewer, and have clarified this by amending the figure 7 legend, as follows: "…**p <0.01 compared to $Casr^{+/+}$ mice at respective glucose and Ca^{2+}_o concentrations…"*

Figure 9:

1. In the legend on page 28, line 1, please change "12 mM (12G) and 20 mM (20G)" to "6 mM (6G)".

We are grateful to the reviewer for detecting this error, and have amended the glucose concentrations to "…1 mM (1G) and 6 mM (6G)…"

2. It is stated that p-values are compared to Casr+/+ mice at respective glucose concentrations. In panel C and D, are the Casr+/+ mice at glucose 6 mM and with tolbutamide being compared to the Casr+/+ mice at glucose 1mM? Please clarify these p-values.

*We thank the reviewer for this comment, and confirm that the Casr+/+ mice at 6 mM glucose and with tolbutamide are being compared to the Casr+/+ mice at 1mM glucose. We have amended the figure 9 legend to clarify this, as follows: "…*p <0.05, **p <0.01 compared to respective α-cells at 1 mM glucose…"*

We thank the editors and reviewers for their comments and have aimed to comply with all of the requested revisions. We will be glad to provide further information if required.

With best wishes,

Yours sincerely,

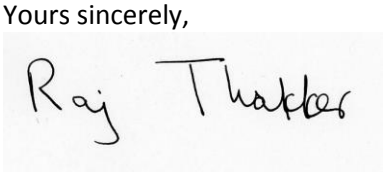

Professor R V Thakker
May Professor of Medicine

Mutant mice with calcium-sensing receptor (CaSR) activation have hyperglycemia, that is rectified by calcilytic therapy

Valerie N. Babinsky[1]*, Fadil M. Hannan[1,2]*, Reshma D. Ramracheya[1]*, Quan Zhang[1]*, M. Andrew Nesbit[1,3], Alison Hugill[4], Liz Bentley[4], Tertius A. Hough[4], Elizabeth Joynson[4], Michelle Stewart[4], Abhishek Aggarwal[5], Maximilian Prinz-Wohlgenannt[5], Caroline M. Gorvin[1], Enikö Kallay[5], Sara Wells[4], Roger D. Cox[4], Duncan Richards[6], Patrik Rorsman[1], Rajesh V. Thakker[1]

*V.N.B., F.M.H., R.R., and Q. Z. contributed equally to the study

[1]Radcliffe Department of Medicine, Oxford Centre for Diabetes, Endocrinology and Metabolism (OCDEM), University of Oxford, Oxford, UK.

[2]Department of Musculoskeletal Biology, Institute of Ageing and Chronic Disease, University of Liverpool, Liverpool, UK.

[3]Biomedical Sciences Research Institute, Ulster University, Coleraine, UK.

[4]MRC Mammalian Genetics Unit and Mary Lyon Centre, MRC Harwell Institute, Harwell Science and Innovation Campus, UK.

[5]Department of Pathophysiology and Allergy Research, Medical University of Vienna, Vienna, AUT.

[6]GlaxoSmithKline Clinical Unit, Cambridge, UK.

Short title: CaSR activation in mice causes hyperglycemia

Key words: G-protein-coupled receptors, calcium, insulin, glucagon, diabetes

Corresponding author and person to whom reprints should be addressed:

Prof Rajesh V. Thakker

Academic Endocrine Unit, Radcliffe Department of Medicine, Oxford Centre for Diabetes, Endocrinology and Metabolism (OCDEM), Churchill Hospital, Oxford OX3 7LJ, UK.

Phone: +44 1865 857501; Fax: +44 1865 857502

Email: rajesh.thakker@ndm.ox.ac.uk

This work was supported by the UK Medical Research Council (MRC) programme grants - G9825289 and G1000467 (to M.A.N., F.M.H., and R.V.T.), and by the UK MRC (to A.H., L.B., T.A.H., E.J., M.S., S.W., and R.D.C. (MC_U142661184)); GlaxoSmithKline (to F.M.H. and R.V.T. for ronacaleret *in vivo* studies); National Institute for Health Research (NIHR) Oxford Biomedical Research Centre Programme (to M.A.N. and R.V.T.); V.N.B. and A.A. were Marie Curie Early Stage Researchers funded by an EU Marie Curie ITN grant (FP7-264663; to R.V.T and E.K); R.D.R. and Q.Z. hold RD Lawrence Diabetes UK Fellowships; P.R. is a Wellcome Trust Senior Investigator; R.V.T. is a Wellcome Trust Senior Investigator and NIHR Senior Investigator

Disclosure summary: F.M.H. and R.V.T. have received grant funding from GlaxoSmithKline and NPS/Shire Pharmaceuticals for studies involving the use of calcium-sensing receptor allosteric inhibitors. R.V.T. has also received grants from Novartis Pharma AG and the Marshall Smith Syndrome Foundation for unrelated studies. Duncan Richards is an employee of GlaxoSmithKline.

Abstract

The calcium-sensing receptor (CaSR) is a family C G-protein-coupled receptor (GPCR) that plays a pivotal role in extracellular calcium homeostasis. The CaSR is also highly expressed in pancreatic islet α- and β-cells that secrete glucagon and insulin, respectively. To determine whether the CaSR may influence systemic glucose homeostasis, we characterized a mouse model with a germline gain-of-function CaSR mutation, Leu723Gln, referred to as *Nuclear flecks* (*Nuf)*. Heterozygous- ($Casr^{Nuf/+}$) and homozygous-affected ($Casr^{Nuf/Nuf}$) mice were shown to have hypocalcemia in association with impaired glucose tolerance and insulin secretion. Oral administration of a CaSR antagonist compound, known as a calcilytic, rectified the glucose intolerance and hypoinsulinemia of $Casr^{Nuf/+}$ mice, and ameliorated glucose intolerance in $Casr^{Nuf/Nuf}$ mice. *Ex vivo* studies showed $Casr^{Nuf/+}$ and $Casr^{Nuf/Nuf}$ mice to have reduced pancreatic islet mass and β-cell proliferation. Electrophysiological analysis of isolated $Casr^{Nuf/Nuf}$ islets showed CaSR activation to increase the basal electrical activity of β-cells independently of effects on the activity of the ATP-sensitive K^+ (K_{ATP}) channel. $Casr^{Nuf/Nuf}$ mice also had impaired glucose-mediated suppression of glucagon secretion, which was associated with increased numbers of α-cells and a higher α-cell proliferation rate. Moreover, $Casr^{Nuf/Nuf}$ islet electrophysiology demonstrated an impairment of α-cell membrane depolarization in association with attenuated α-cell basal K_{ATP} channel activity. These studies indicate that the CaSR activation impairs glucose tolerance by a combination of α- and β-cell defects and also influences pancreatic islet mass. Moreover, our findings highlight a potential application of targeted CaSR compounds for modulating glucose metabolism.

Précis: Mice with a germline gain-of-function CaSR mutation have hypoinsulinemia, hyperglucagonemia, reduced pancreatic islet mass; and impaired glucose tolerance, which is rectifiable by calcilytic therapy.

Introduction

Glucose homeostasis is tightly regulated by the joint actions of insulin and glucagon, which are secreted from the pancreatic islet β- and α-cells, respectively (1,2). Diabetes mellitus is a bihormonal disorder which affects >330 million people worldwide, and is characterized by reduced insulin secretion and aberrant glucagon secretion, which arises from alterations in islet function as well as mass (1,2). G-protein-coupled receptors (GPCRs), which comprise the largest superfamily within the human proteome and are targeted by 40% of all currently approved drugs (3), facilitate the effects of diverse extracellular stimuli, ranging from fatty acids to neurotransmitters and gut hormones, on α- and β-cells and represent an exploitable target for the modulation of glucose homeostasis (4,5). The extracellular calcium (Ca^{2+}_o)-sensing receptor (CaSR) is a family C GPCR that plays a key role in the parathyroid and renal regulation of Ca^{2+}_o homeostasis by: coupling to intracellular signal transduction cascades that include the $G_{q/11}$-mediated stimulation of phospholipase C (PLC), which increases inositol 1,4,5-trisphosphate (IP_3), thereby leading to a rapid rise in cytosolic calcium (Ca^{2+}_i) concentrations; and activating the MAPK pathway (6). The CaSR is also highly expressed in pancreatic islet α- and β-cells (7,8), and studies involving isolated human islets and insulin-secreting cell lines have shown that activation of the CaSR following exposure to elevated Ca^{2+}_o concentrations or allosteric activators triggers transient stimulations of insulin and glucagon secretion, which were associated with upregulation of PLC and MAPK-mediated signaling responses (8-10). Moreover, a study involving wild-type (WT) mice has demonstrated pancreatic islet CaSR expression to be associated with insulin secretion *in vivo* (11). However, the role of this GPCR in systemic glucose homeostasis is unclear. For example, one patient-based association study has reported a common coding-region CaSR gene variant to be an independent determinant of plasma glucose concentrations (12), whilst another study of patients with familial hypocalciuric hypercalcemia (FHH), which is caused by germline loss-of-function CaSR mutations, did not reveal any alterations in glucose tolerance or insulin secretion (13). However, it may be that gain-of-function CaSR mutations, which cause autosomal dominant hypocalcemia (ADH) (14), are associated with abnormalities of glucose homeostasis and not FHH-associated loss-of-function CaSR mutations. To investigate this possibility,

we have evaluated glucose tolerance and pancreatic islet function in a mouse model for ADH due to a germline gain-of-function CaSR mutation, Leu723Gln, referred to as *Nuclear flecks* (*Nuf*) because the mouse was initially identified to have cataracts (15,16). Our analysis of these *Nuf* mice has demonstrated a role for the CaSR in glucose homeostasis

Materials and Methods

Animals

All study animals were litter-mates aged between 20-28 weeks and kept in accordance with Home Office welfare guidance in an environment controlled for light (12 hours light and dark cycle), temperature (21 ± 2°C) and humidity (55 ± 10%) at the Medical Research Council (MRC) Harwell Centre. Mice had free access to water (25 ppm chlorine) and were fed *ad libitum* on a commercial diet (RM3, Special Diet Services, UK) that contained 1.24% calcium, 0.83% phosphorus and 2948 IU/kg of vitamin D. *Nuf* mice were maintained on the inbred 102/H background, which is a substrain bred at the Mary Lyon Centre (Harwell, UK (15,16). Animal studies were carried out in accordance with GlaxoSmithKline policy on the care, welfare and treatment of animals, approved by the MRC Harwell Institute Ethical Review Committee, and were licensed under the Animal (Scientific Procedures) Act 1986, issued by the UK Government Home Office Department (PPL30/2752).

Compounds

Ronacaleret, which is also known as SB-751689, was provided by GlaxoSmithKline and dissolved in a 20% aqueous solution of 2-hydroxypropyl-β-cyclodextrin (Sigma-Aldrich, catalog no. H107) prior to use in *in vitro* and *in vivo* studies.

Cell culture and transfection

Human embryonic kidney (HEK) 293 cells were cultured in high-glucose DMEM (Invitrogen) supplemented with 10% fetal bovine serum (FBS), as described (17). WT (Leu723) and mutant (Gln723) CaSR-pEGFP-N1 constructs were generated, as reported (16), and transiently transfected into HEK293 cells using Lipofectamine Plus (Invitrogen), as described (16). Successful transfection of WT and mutant CaSR proteins were confirmed was confirmed by visualising green fluorescence protein (GFP) fluorescence using an Eclipse E400 fluorescence microscope with an epifluorescence filter, and images were captured using a DXM1200C digital camera and NIS Elements software (Nikon), as described (17).

Measurement of $Ca^{2+}{}_i$ responses

The effect of ronacaleret on the $Ca^{2+}{}_i$ responses of CaSR-expressing cells was assessed by a flow cytometry-based assay, as reported (17,18). In brief, 48 hours after transfection, the cells were harvested, washed in calcium- and magnesium-free Hank's balanced salt solution (HBSS, Invitrogen) and loaded with 1μg/ml indo-1-acetoxymethylester (Indo-1-AM) (Molecular Probes) for 1 hour at 37 $^{\circ}$ C (17,18). After the removal of free dye, the cells were resuspended in calcium- and magnesium-free HBSS and maintained at 37°C. Transfected cells were incubated with either a 20% aqueous solution of 2-hydoxypropyl- β -cyclodextrin (vehicle), or ronacaleret at concentrations of 20 and 40nM for 1 hour, as described (18). Flow cytometry was performed using a Beckman Coulter MoFlo XDP equipped with JDSUY Xcyte UV Laser and a Coherent Sapphire 488 Laser with a 550LP dichroic mirror and 580/30 bandpass filter (17). Single cells were isolated and stimulated by sequentially adding calcium to increase the $Ca^{2+}{}_o$ concentration ($[Ca^{2+}]_o$) in a stepwise manner from 0-15 mM. The baseline fluorescence ratio was measured for 2 min, the fluorescence ratio compared to the time was recorded and data were collected for 2 min at each $[Ca^{2+}]_o$, as described (17,18). Cytomation Summit software was used to determine the peak mean fluorescence ratio of the transient response after each individual stimulus, which was expressed as a percentage normalized response (17,18). Nonlinear regression of the concentration-response curves was performed with GraphPad Prism (GraphPad) to calculate the half-maximal (EC_{50}) responses for each separate experiment (17).

Effect of ronacaleret on the glucose tolerance of Nuf mice

Ronacaleret (20 mg/ml) or drug vehicle was administered by twice daily oral gavage to mice over a 5-day period. The mice were then tested using the international mouse phenotyping consortium (IMPC) glucose tolerance test protocol (https://www.mousephenotype.org/impress/protocol/87/7). Briefly, mice were fasted for 16 hours, and a blood sample obtained before IP administration of a 2g/kg glucose load. Subsequent blood samples were taken at 30, 60 and 120 min for plasma glucose and glucagon measurements; or at 10, 20, and 30 min for plasma insulin measurements, as described (19).

Body composition analysis

Fat and lean body mass of non-anaesthetized live mice were measured using the Echo-MRI Analyzer system (Echo Medical Systems, Houston, TX), as described (20).

Islet insulin and glucagon secretion

Pancreatic islets were isolated from whole mouse pancreata by collagenase digestion and separated from the suspension, as described (19). Islets were used for secretion experiments within 2 hours of isolation. Batches of 13 size-matched islets were incubated for 1 hour at 37°C in 0.3 ml of modified Krebs-Ringer buffer containing 2mg/ml BSA, 1.6 mM $CaCl_2$ and 3mM glucose, followed by a 1 hour incubation in 0.3 ml of the same Krebs-Ringer buffer supplemented with 1, 6 or 20 mM glucose, as described (21). A Krebs-Ringer buffer containing 0.8 mM $CaCl_2$ was used to evaluate the effect of lowering the $[Ca^{2+}]_o$ on islet hormone secretion. The supernatant was used for measurement of secreted insulin and glucagon, and islets were lysed in cold acid ethanol for measurement of insulin and glucagon content. Insulin and glucagon was determined by radioimmunoassay (Millipore UK Ltd, Livingstone, UK) or using a Rat/Mouse Insulin, Glucagon duplex ELISA (Meso Scale Discovery).

Quantitative RT-PCR

Total RNA from isolated islets was extracted using an RNeasy mini-kit (Qiagen) and cDNA was generated by the Superscript II enzyme (Invitrogen), as described (19). QuantiTect primer assays were used to amplify selected genes (*Arx, Ccnd2, Foxm1, Foxo1, Irx2, Nkx6, Pax4, Pax6, Pdx1, Tcf7l2*), which were analyzed by quantitative RT-PCR (qRT-PCR) using SYBR Green (Qiagen) on the StepOnePlus qRT-PCR system (Life Technologies), as described (22). The ΔΔCt method was used to calculate fold change alterations in gene expression, relative to a housekeeping panel comprising the *Actb, Eef1b2, and Gapdh* genes (22).

Biochemical analysis

Blood samples were collected from the lateral tail vein of study mice following application of topical local anesthesia, as reported (23), or collected from the retro-orbital vein under isoflurane terminal

anesthesia. Plasma was separated by centrifugation at 5000 g for 10 min at 8°C, and analysed for calcium and albumin on a Beckman Coulter AU680 analyzer, as described (15). Plasma calcium was adjusted for variations in albumin concentrations using the formula: (plasma calcium (mmol/l) – [(plasma albumin (g/l) – 30) x 0.02], as reported (23). Plasma glucose concentrations were measured using an Analox GM9 analyzer, as described (19). Plasma insulin concentrations were measured using a Rat/Mouse Insulin ELISA (Millipore), as described (19), and plasma glucagon concentrations measured using a Rat/Mouse Glucagon ELISA (Mercodia).

Islet electrophysiology

Electrical activity was measured from α- and β-cells within intact mouse islets using the perforated-patch technique, as described (24), and all measurements were obtained at 34˚C. Islets were immobilised using a wide-bore glass suction pipette (24) and perfused with modified Krebs-Ringer solution (140 mM NaCl, 3.6 mM KCl, 1.5 mM $CaCl_2$, 0.5 mM $MgSO_4$, 10 mM HEPES, 0.5 mM NaH_2PO_4 and $NaHCO_3$ at pH 7.4 with NaOH, and glucose as indicated), as reported (25). A Krebs-Ringer solution containing 0.75 mM $CaCl_2$ was used to evaluate the effect of lowering the $[Ca^{2+}]_o$ on islet electrical activity. The solution within the pipet contained 76 mM K_2SO_4, 10 mM KCl, 10 mM NaCl, 1 mM $MgCl_2$, 5 mM HEPES (pH 7.35 using KOH) (24). To perforate the cell membrane, amphotericin B (6 μg/ml) was added to the intracellular buffer. The conductance of the β-cell ATP-sensitive K^+ (K_{ATP}) channel within intact islets was measured using the perforated patch clamping technique following exposure to different glucose concentrations or to tolbutamide (24). During the K_{ATP} channel conductance studies, β-cells were held at -70 mV, and K^+ currents were evoked by exposing the cells to alternating 50 ms pulses of -60 or -80 mV (25). Islet cell types were established by their electrical activity in response to glucose, and cells that were electrically active at 1 mM glucose were identified as α-cells (26). Furthermore, β-cells were distinguished from non-β-cells by the absence of a voltage-gated Na^+-current when a transient pulse from -70 mV to 0 mV was applied (21). Measurements were undertaken in individual islets using EPC-10 patch-clamp amplifier (HEKA Electronics, http://www.heka.com/) and Pulse software (version 8.50) as described previously (24).

Islet area analysis

Mouse pancreata were fixed in 10% neutral buffered formalin, mounted longitudinally and paraffin embedded, as described (19). Serial sections (4.5µm) were cut and every 10th section stained with H&E, as described (19). Images of ≥10 H&E-stained sections per mouse were acquired at a 20x magnification using the semi-automated TissueFax slide-scanning microscope (TissueGnostics, Austria), as described (27). Islets were identified and islet area, size and number quantified using HistoQuest software (TissueGnostics, Austria) (27). Islet area was normalised to the total section area and to body weight, and islet size was calculated by dividing the total islet area per section by the number of islets on the same section.

Islet immunohistochemistry

Immunohistochemistry was undertaken using paraffin-embedded pancreatic sections that had been subjected to heat-induced epitope retrieval in citrate buffer (pH 6.0), followed by blocking in 10% donkey serum for 1 hour. Primary antibodies used for insulin, glucagon, and Ki-67 staining were guinea pig anti-insulin (1:200, abcam - ab7842 (RRID: AB_306130)) rabbit anti-glucagon (1:200, abcam - ab92517 (RRID: AB_10561971)), and rabbit anti-Ki67 (1:500, abcam - ab15580 (RRID: AB_443209)), respectively. Secondary antibodies used were donkey anti-guinea pig (Jackson: 706-225-148, Cy2 (RRID: AB_2340467)) 1: 100, and donkey anti-rabbit (Jackson: 711-165-152, Cy3 (RRID: AB_2307443)) 1:500, in PBS. Sections were mounted in prolong Gold anti-fade reagent containing DAPI (Life Technologies). Images of whole sections were acquired using the TissueFax slide-scanning microscope TissueFax (TissueGnostics, Austria), as described (27). Quantification of immunofluorescence signals was undertaken using the semi-automated intensity detection function of the TissueQuest software (TissueGnostics, Austria), as described (27). The numbers of α- and β-cells within individual islets were quantified using the cell-based analysis profile of the TissueQuest software (27), and normalized to the total islet area, and reported as percentage of the mean numbers of *Casr*$^{+/+}$ α- and β-cells, respectively.

Statistical analysis

The *in vitro* studies involved two separate transfection experiments and 8-9 technical assays. Statistical comparisons of the EC_{50} responses were undertaken using the *F*-test (17,18). For the *in vivo* and *ex vivo* studies, the Mann-Whitney *U* test was used to compare differences between two groups, and the Kruskal-Wallis test was used to compare multiple groups. An unpaired Student's t-test was used to compare groups with small sample sizes ($n < 5$), as reported (28). All analyses were undertaken using GraphPad Prism (GraphPad), and a value of $p < 0.05$ was considered significant for all analyses.

Results

Nuf mice have impaired glucose tolerance that is ameliorated by a CaSR allosteric modulator

To establish whether the gain-of-function CaSR mutation in *Nuf* mice may be associated with alterations in glucose homeostasis, IP glucose tolerance testing (IPGTT) was performed on WT *($Casr^{+/+}$)*, heterozygous- ($Casr^{Nuf/+}$) and homozygous-affected ($Casr^{Nuf/Nuf}$) mice aged 20-28 weeks that had been fasted for 16 hours. Plasma glucose concentrations were measured at 0, 30, 60 and 120 min following an IP 2g/kg glucose bolus injection. Male and female $Casr^{Nuf/+}$ and $CasrCasr^{Nuf/Nuf}$ mice had elevated plasma glucose concentrations at 30 and 60 min, which were significantly ($p < 0.01$) greater than those of respective $Casr^{+/+}$ mice (Figure 1A-B). The impaired glucose tolerance was not associated with any alterations in body weight, or in fat or lean mass (Supplemental Figure 1). To test whether the impaired glucose tolerance of *Nuf* mice may be associated with abnormalities of insulin secretion *in vivo*, an IPGTT was conducted with plasma samples collected for insulin measurement at 0, 10, 20 and 30 min. Plasma insulin concentrations of male and female $Casr^{+/+}$ mice increased two-fold at 10 min after an IP 2g/kg glucose bolus injection (Figure 1C-D). However, male affected $Casr^{Nuf/+}$ and $Casr^{Nuf/Nuf}$ mice showed significantly reduced plasma insulin concentrations at 10 and 20 min following glucose administration (Figure 1C); whereas only female $Casr^{Nuf/Nuf}$ mice showed significantly reduced insulin concentrations at 20 min (Figure 1D), compared to respective $Casr^{+/+}$ mice. Affected male $Casr^{Nuf/Nuf}$ mice were also shown to have an inadequate suppression of plasma glucagon concentrations at the 30 min time-point during a 120 min IPGTT (Figure 1E), whereas female $Casr^{Nuf/Nuf}$ mice had significantly raised plasma glucagon concentrations at 120 min (Figure 1F). No significant differences in the glucose, insulin or glucagon responses were noted between male and female mice (Supplemental Figure 2).

To investigate if the impaired glucose tolerance of *Nuf* mice, which have the Leu723Gln gain-of-function CaSR mutation, could be corrected by a selective CaSR negative allosteric modulator i.e. calcilytic agent, we assessed the *in vitro* and *in vivo* effects of ronacaleret, a calcilytic compound (29). For the *in vitro* studies, HEK293 cells were transiently transfected with WT (Leu723) or mutant (Gln723) *CASR*-pEGFP-N1 constructs, which express the CaSR protein fused to the N-terminus of

enhanced GFP (EGFP) (16), and the effect of ronacaleret on the responses of Ca^{2+}_i concentrations to alterations in $[Ca^{2+}]_o$ was assessed. HEK293 cells expressing the mutant Gln723 CaSR (Figure 2A) were shown to have a leftward shift of the concentration-response curve (Figure 2B) with a significant reduction in EC_{50} (2.63 ± 0.08 mM), compared to WT (2.92 ± 0.06 mM; $p < 0.01$) (Figure 2C), consistent with a gain-of-function, as reported (16). A dose titration of ronacaleret revealed 20 nM and 40 nM concentrations of this calcilytic compound to normalise the EC_{50} values and shift in the concentration-response curve of mutant Gln723-expressing cells (Figure 2B-C). Glucose has recently been reported to lead to allosteric activation of the CaSR (30), and we investigated the effect of alterations in glucose concentrations on the Ca^{2+}_i responses of WT and *Nuf* mutant Gln723 CaSRs, which were stably expressed in HEK293 cells (Supplemental Figure 3). Our findings showed that altering the glucose concentration from 3 mM to 25 mM had no effect on the EC_{50} values of cells stably expressing WT or *Nuf* mutant Gln723 CaSRs, whereas the addition of 40 nM ronacaleret significantly increased the EC_{50} values of these cells (Supplemental Figure 3). To determine whether amelioration of CaSR gain-of-function by ronacaleret, may lead to an improvement in glucose tolerance *in vivo*, we administered this calcilytic agent to *Nuf* mice. Male and female $Casr^{+/+}$, $Casr^{Nuf/+}$ and $Casr^{Nuf/Nuf}$ mice were given ronacaleret or drug vehicle for 5-days by twice daily oral-gavage. Ronacaleret was administered at a dose of 90 mg/kg, as pilot studies had shown this dose to increase plasma calcium concentrations and to be well tolerated in $Casr^{+/+}$ mice. Untreated $Casr^{Nuf/+}$ and $Casr^{Nuf/Nuf}$ mice were shown to be significantly hypocalcemic compared to $Casr^{+/+}$ mice, and $Casr^{Nuf/Nuf}$ mice had significantly lower plasma calcium concentrations than $Casr^{Nuf/+}$ mice (Figure 2D-E). Ronacaleret treatment significantly ($p < 0.01$) increased plasma calcium concentrations in male and female $Casr^{+/+}$, $Casr^{Nuf/+}$ and $Casr^{Nuf/Nuf}$ mice compared to respective untreated mice (Figure 2D-E). Ronacaleret treatment normalised the plasma calcium concentrations of male and female $Casr^{Nuf/+}$ mice (Figure 2D-E). However, the plasma calcium concentrations of treated $Casr^{Nuf/Nuf}$ mice remained significantly reduced compared to untreated $Casr^{+/+}$ mice (Figure 2D-E). Ronacaleret treatment had no effect on the plasma glucose concentrations of male and female $Casr^{+/+}$ mice (Figures 3 and 4), but significantly ($p < 0.05$) improved glucose tolerance in male and female $Casr^{Nuf/+}$ and $Casr^{Nuf/Nuf}$ mice compared to respective mice treated with the drug vehicle alone (Figures 3 and 4). Moreover, gender

differences were noted, as ronacaleret normalised plasma glucose concentrations at 30 min in male *Casr*$^{Nuf/+}$ mice, but only at 60 min in female *Casr*$^{Nuf/+}$ mice (Figures 3 and 4). Ronacaleret treatment had no effect on the plasma insulin concentrations of male and female *Casr*$^{+/+}$ mice (Figures 3 and 4), but significantly increased the plasma insulin concentrations of male and female *Casr*$^{Nuf/+}$ mice compared to untreated *Casr*$^{Nuf/+}$ mice (Figures 3 and 4). Ronacaleret treatment did not alter plasma insulin concentrations in male and female *Casr*$^{Nuf/Nuf}$ mice (Figures 3 and 4), and had no significant effect on the plasma glucagon concentrations of male and female *Casr*$^{+/+}$, *Casr*$^{Nuf/+}$ or *Casr*$^{Nuf/Nuf}$ mice (Figures 3 and 4). No significant differences were noted between the biochemical responses of ronacaleret-treated male and female mice (Supplemental Figure 3). To evaluate the mechanisms underlying these alterations of glucose tolerance, and plasma insulin and glucagon concentrations in *Nuf* mice, further *ex vivo* and electrophysiological studies were undertaken. As no significant differences had been observed for the glucose, insulin and glucagon responses of male and female mice, the *ex vivo* data were combined for males and females.

Pancreatic islet size and proliferation

We assessed for alterations in islet morphology by undertaking histological analysis of whole pancreases from adult *Casr*$^{+/+}$, *Casr*$^{Nuf/+}$ and *Casr*$^{Nuf/Nuf}$ mice. This revealed that the overall architecture of *Casr*$^{Nuf/+}$ and *Casr*$^{Nuf/Nuf}$ islets was similar to that in *Casr*$^{+/+}$ mice (Figure 5A). However, islet area, which was normalised to body weight, was reduced by >40% in *Casr*$^{Nuf/+}$ and *Casr*$^{Nuf/Nuf}$ mice (Figure 5B), and this was associated with significant decreases in islet numbers and mean islet size (Figure 5C-D). To assess, whether the reduced islet area may also be associated with alterations in the numbers of β-cells or α-cells, whole pancreas sections were immunostained for insulin and glucagon (Figure 5E). Individual islets from *Casr*$^{Nuf/Nuf}$ mice had 5-10% fewer β-cells ($p < 0.05$) and ~20% more α-cells than *Casr*$^{+/+}$ islets ($p < 0.05$) (Figure 5F-G). To investigate whether the reduction in β-cells and increase in α-cells were caused by alterations in cellular proliferation, whole pancreas sections were immunostained with the proliferation marker Ki-67. (Figure 5H). The percentage of proliferating insulin-positive β-cells in *Casr*$^{Nuf/Nuf}$ mice was found to be significantly decreased ($p < 0.05$), whereas the percentage of proliferating insulin-negative cells (which are predominantly α-cells) was

significantly increased when compared to respective *Casr*$^{+/+}$ islets (Figure 5I-J). Quantitative RT-PCR analysis utilising RNA from isolated *Casr*$^{+/+}$ and *Casr*$^{Nuf/Nuf}$ islets revealed that these changes in β-cell and α-cell proliferation were not associated with significant alterations in the expression of genes regulating islet mass such as *Foxo1*, *Foxm1*, *Ngn3*, and *Tcf7l2* (31-34), which promote β-cell proliferation; or in the expression of genes such as *Arx* and *Irx2* (35), which influence α-cell proliferation (Supplemental Figure 4).

Insulin and glucagon secretion from isolated islets

To determine whether *Nuf* mice have alterations in pancreatic islet insulin secretion, size-matched islets were isolated from *Casr*$^{+/+}$ and *Casr*$^{Nuf/Nuf}$ mice, and exposed to low (1 mM), physiological (6 mM) or high (20 mM) glucose concentrations in the presence of 1.6 mM $[Ca^{2+}]_o$, which represents a physiological $[Ca^{2+}]_o$ (36). The insulin content of isolated *Casr*$^{Nuf/Nuf}$ islets was not significantly different from isolated *Casr*$^{+/+}$ islets (Figure 6A). Measurement of insulin in the supernatant of islets following glucose stimulation did not reveal any impairment in the insulin secretory responses of isolated *Casr*$^{Nuf/Nuf}$ islets compared to *Casr*$^{+/+}$ islets (Figure 6B). We also investigated whether glucagon secretion may be altered in *Nuf* mouse islets. Compared to *Casr*$^{+/+}$ islets, there was a >30% increase in the glucagon content (Figure 6C) of *Casr*$^{Nuf/Nuf}$ islets. Increasing glucose from 1 to 6 mM resulted in a 60% reduction of glucagon secretion from isolated *Casr*$^{+/+}$ islets (Figure 6D). In contrast, islets from *Casr*$^{Nuf/Nuf}$ mice exhibited a lack of glucose-induced suppression of glucagon release (Figure 6D), which is consistent with that observed in islets from type 2 diabetic patients (37). To investigate whether the reduced plasma insulin concentrations of *Nuf* mice may have been a consequence of their hypocalcemia, insulin secretion from isolated islets was measured following exposure to 0.8 mM $[Ca^{2+}]_o$, which is similar to the plasma calcium concentrations observed in *Casr*$^{Nuf/Nuf}$ mice (15,16). Altering the $[Ca^{2+}]_o$ had no effect on insulin secretion in the presence of low (1 mM) glucose concentrations (Figure 6E). However, exposure to low (0.8 mM) $Ca^{2+}{}_o$ impaired insulin secretion from *Casr*$^{+/+}$ and *Casr*$^{Nuf/Nuf}$ islets in the presence of high (20 mM) glucose concentrations (Figure 6E). Exposure to low (0.8 mM) $Ca^{2+}{}_o$ increased glucagon secretion from

Casr$^{+/+}$ islets at 20 mM glucose, but had no effect on glucagon secretion from *Casr*$^{Nuf/Nuf}$ islets (Figure 6F).

Electrophysiological studies of isolated islets. We investigated for alterations in β-cell electrical activity by recording the membrane potential of β-cells within intact *Casr*$^{+/+}$ and *Casr*$^{Nuf/Nuf}$ islets upon treatment with varying (1 mM, 12 mM or 20 mM) concentrations of glucose, or to tolbutamide, which is an ATP-sensitive K^+ (K_{ATP}) channel blocker (26). The electrophysiological experiments were undertaken at 1.5 mM $[Ca^{2+}]_o$, as described (25), and the effect of lowering the $[Ca^{2+}]_o$ on β-cell electrical activity was evaluated at 0.75 mM $[Ca^{2+}]_o$, which is in keeping with the plasma calcium concentrations of *Casr*$^{Nuf/Nuf}$ mice (15,16). Analysis of membrane potentials showed β-cells from *Casr*$^{+/+}$ mice (i.e. WTs) to be hyperpolarised (-76 ± 2 mV) and electrically silent at 1 mM glucose concentrations (Figure 7A). In contrast, *Casr*$^{Nuf/Nuf}$ β-cells were significantly depolarized (-63 ± 5 mV, $p < 0.01$) at 1 mM glucose, and >40% (4 out of 9) of cells were electrically active with low frequency action potential firing (Figure 7A). The depolarization and hyperactivity of *Casr*$^{Nuf/Nuf}$ β-cells was rectified by lowering $[Ca^{2+}]_o$ from 1.5 mM to 0.75 mM (Figure 7B-C). At stimulatory glucose concentrations (12 or 20 mM) or following application of tolbutamide, both *Casr*$^{+/+}$ and *Casr*$^{Nuf/Nuf}$ β-cells were depolarized and firing action potentials (Figure 7A-B), and the level of the depolarization was not altered in *Casr*$^{Nuf/Nuf}$ β-cells (Figure 7C). However, the peak of action potential evoked by 20 mM glucose in *Casr*$^{Nuf/Nuf}$ β-cells was significantly reduced compared to *Casr*$^{+/+}$ β-cells (Figure 7D). The anti-peak potential and firing frequency were not affected by the expression of the *Casr* mutation or variation in $[Ca^{2+}]_o$ (Figure 7E-F). Based on the observation that *Casr*$^{Nuf/Nuf}$ β-cells were significantly depolarized at 1 mM glucose, we postulated that the CaSR may influence the K_{ATP} channel, which plays a central role in regulating the membrane potential of β-cells (1). We therefore measured resting conductance, which predominantly reflects K_{ATP} channel activity, of *Casr*$^{+/+}$ and *Casr*$^{Nuf/Nuf}$ β-cells in the presence of 1, 12 or 20 mM glucose, or with tolbutamide. These studies showed β-cell resting conductance to be comparable between genotypes (Figure 8A-B). However, the holding current measured at – 70 mV in *Casr*$^{Nuf/Nuf}$ β-cells when K_{ATP} channel activity was suppressed by 20 mM glucose or tolbutamide was significantly greater than in *Casr*$^{+/+}$ β-cells (Figure 8C-D), and

its contribution likely accounts for the more depolarized membrane potential and action potential firing in *Casr*$^{Nuf/Nuf}$ β-cells exposed to 1 mM glucose (Figure 7A).

To determine whether *Nuf* mice may also have alterations in α-cell electrical activity, membrane potentials were recorded in intact islet α-cells, as described (26). In agreement with previous reports (37), *Casr*$^{+/+}$ α-cells were shown to be electrically active at 1 mM glucose (Figure 9A). The addition of 6 mM glucose led to a small but statistically significant ($p < 0.01$) depolarisation and reduction in action potential peak (Figure 9A). *Casr*$^{Nuf/Nuf}$ α-cells were also electrically active at 1 mM glucose (Figure 9B), but did not depolarise when glucose was increased to 6 mM (Figure 9B-C) and there was no change in the action potential peak (Figure 9B and 9D). The addition of tolbutamide led to membrane depolarization in both *Casr*$^{+/+}$ and *Casr*$^{Nuf/Nuf}$ α-cells (Figure 9A-B) but the magnitude of the depolarizing effect was reduced in *Casr*$^{Nuf/Nuf}$ α-cells (Figure 9C). Tolbutamide also decreased the action potential peak of *Casr*$^{+/+}$ α-cells, but had no significant effect on the action potential peak of *Casr*$^{Nuf/Nuf}$ α-cells (Figure 9A-B and 9D). There were no significant differences in the action potential frequency between *Casr*$^{+/+}$ and *Casr*$^{Nuf/Nuf}$ α-cells and this was not affected by varying glucose or with the addition of tolbutamide (Figure 9E).

Discussion

Our studies have shown an *in vivo* role for the CaSR in glucose homeostasis, and in the regulation of pancreatic islet mass and islet hormone secretion. Thus, *Nuf* mice with a gain-of-function CaSR mutation exhibited impaired glucose tolerance, which was associated with reduced pancreatic islet mass and hypoinsulinemia, as well as a lack of glucose-mediated suppression of glucagon secretion. Moreover, these findings indicate that ADH-causing mutations of the CaSR, which lead to a gain-of function (14), may perturb systemic glucose homeostasis, and this contrasts with FHH-causing loss-of-function CaSR mutations, which have been shown to not influence glucose tolerance or insulin secretion (13). Furthermore, these findings suggest that a common coding-region CaSR SNP (Ala986Ser), which was reported in association with raised plasma glucose concentrations in a patient-based study (12), may have altered CaSR function in tissues involved in systemic glucose regulation. However, impaired glucose tolerance or diabetes has not been reported in ADH patients to-date, and detailed investigations of glucose homeostasis in humans are warranted.

Although our studies showed CaSR activation to influence plasma glucose concentrations, we did not observe any effect of extracellular glucose on the acute signalling responses of WT or mutant Nuf CaSRs in vitro. Our findings are consistent with results obtained by other groups (personal communications from A. Conigrave and D. Ward), but contrast with a recent study, which showed that raising the glucose concentration from 3 to 5 mM increased the Ca^{2+}_i responses of stably expressing HEK293-CaSR cells in the presence of Ca^{2+}_o (30). This recent study, which showed glucose to act as a CaSR allosteric activator, measured Ca^{2+}_i responses in single cells using the fluo-8 calcium binding dye (30), whereas, our study measured Ca^{2+}_i responses in populations of HEK293-CaSR cells using the fluo-4 calcium binding dye; and these methodological differences may be contributors to the contrasting observations of these two studies.

The CaSR is a therapeutic target for calcitropic diseases (14,38), and our studies involving the administration of ronacaleret, which is a calcilytic compound, to *Nuf* mice, showed that pharmacological modulation of the CaSR may also alter plasma glucose concentrations. Ronacaleret treatment rectified the hypocalcemia of heterozygous-affected ($Casr^{Nuf/+}$) mice and this was associated

with an increase in plasma insulin concentrations. Thus, these findings suggest that ronacaleret rectified the impaired glucose tolerance and hypoinsulinemia of *Casr*$^{Nuf/+}$ mice by modulating their plasma calcium concentrations, and this is in keeping with our analysis of isolated *Nuf* mice islets, which demonstrated that Ca^{2+}_{o} is required for insulin release, and is also supported by a study showing that patients with chronic hypocalcemia have reduced glucose-stimulated insulin secretion (39). However, ronacaleret treatment also improved the glucose tolerance of homozygous-affected (*Casr*$^{Nuf/Nuf}$) mice without fully normalising their plasma calcium concentrations, or altering plasma insulin or glucagon concentrations. Thus, these studies involving *Casr*$^{Nuf/Nuf}$ mice suggest that ronacaleret likely had additional effects on the glucose tolerance of *Nuf* mice, independently of altering plasma concentrations of calcium, insulin and glucagon. The CaSR is expressed in peripheral tissues such as skeletal muscle and adipose tissue (40,41), and it remains to be established whether ronacaleret treatment may potentially have sensitised these tissues to the actions of insulin, thereby improving glucose tolerance.

Histological analysis revealed *Nuf* mice to have a significant reduction in mean islet area, and these findings may have contributed to their reduced plasma insulin concentrations and impaired glucose tolerance. Indeed, a decrease in pancreatic β-cell mass is considered to be important in the pathogenesis of type 2 diabetes, as highlighted by a study of a mouse model with restricted β-cell expansion, which showed that a 30% reduction in β-cell mass is sufficient to result in impaired glucose tolerance (42). Our histological analyses also revealed individual *Casr*$^{Nuf/Nuf}$ islets to have a significant reduction in the proportion of β-cells compared to *Casr*$^{+/+}$ islets. Thus, these findings indicate that the CaSR may influence pancreatic islet size and the cellular composition of individual islets, and suggest a role for this GPCR in the development and/or maintenance of β-cell mass. In support of this, mouse model studies of the α-2A adrenergic receptor, which is highly expressed in β-cells, have shown GPCR signaling to play a critical role in modulating pancreatic islet mass by inhibiting β-cell proliferation during the perinatal period (42). In keeping with this observation, CaSR activation was also associated with significantly reduced β-cell proliferation in adult *Casr*$^{Nuf/Nuf}$ islets, which may have contributed to the reduced size of *Nuf* mouse islets. However, β-cell proliferation was measured using the Ki67 marker, which shows proliferation over a limited timeframe, and long-term

continuous labeling with the thymidine analog 5-bromo-2-deoxyuridine (BrdU) is required to provide a more accurate assessment of proliferation (43). Moreover, genes reported to be involved in the regulation of islet cell proliferation did not show altered expression in *Casr*$^{Nuf/Nuf}$ islets. Thus, it is possible that the gain-of-function CaSR mutation harbored by *Nuf* mice may have exerted a greater influence on islet size during the perinatal and early postnatal periods, when the β-cell population is undergoing a rapid expansion, and at this key developmental stage, alterations in cellular proliferation can substantially impact on adult β-cell mass and insulin secretory capacity (42). Furthermore, the CaSR may have influenced β-cell apoptosis, which has been shown to contribute to the reduced islet mass in humans with type 2 diabetes (44).

Isolated *Nuf* mouse islets were shown to have alterations in β-cell electrical activity, and *Casr*$^{Nuf/Nuf}$ β-cells were significantly depolarised and electrically active at low glucose concentrations. These findings suggest that the CaSR may influence the basal electrical activity of the β-cell, most likely by increasing background conductance (Figure 8). In support of this, lowering the concentration of Ca^{2+}_o, which represents the major physiological ligand of the CaSR (14), rectified the increased basal activity of *Casr*$^{Nuf/Nuf}$ β-cells. Although the K_{ATP} channel plays an essential role in regulating the β-cell resting membrane potential (45), K_{ATP} channel conductance was not altered in *Casr*$^{Nuf/Nuf}$ β-cells, and the higher background conductance was resistant to the effects of tolbutamide. Thus, the basal hyperactivity of *Casr*$^{Nuf/Nuf}$ β-cells may have been mediated by a K_{ATP} channel-independent mechanism. A previous study has demonstrated that the transient receptor potential (TRP) M4 and TRPM5 ion channels regulate β-cell membrane potential, and activation of these channels leads to increased β-cell electrical activity (25). As TRPM4 and TRPM5 channels have been shown to be activated by $G_{q/11}$-mediated phosphoinositide signaling (25), it is possible that CaSR activation induced depolarisation and hyperactivity of β-cells by enhancing the opening of these channels. However, due to a lack of selective channel blockers, it remains to be established whether CaSR may act via TRPM4 and TRPM5 in β-cells. Interestingly, the increased electrical activity of *Casr*$^{Nuf/Nuf}$ β-cells at 1 mM glucose was not associated with an increase in basal insulin secretion. The release of insulin has been shown to be mediated by a combination of triggering effects (mediated by K_{ATP} channel closure and initiation of action potential firing) and late amplifying effects (exerted at the level of insulin granule exocytosis)

(1). Thus, although *Casr*$^{Nuf/Nuf}$ β-cells generated action potentials at low glucose, this may not necessarily have stimulated insulin secretion. Moreover, the CaSR did not influence the overall responses of β-cells to stimulatory glucose concentrations; however, a reduced spike height of the glucose-induced action potentials in *Casr*$^{Nuf/Nuf}$ β-cells was observed. The generation of action potentials in β-cells is mediated by Ca^{2+} influx through the L-type voltage-dependent Ca^{2+} channel (VDCC) (46), and our observation of altered action potential height provides support for an interaction between the CaSR and L-type VDCC, as has been previously reported (47).

A key finding in this study was the presence of dysregulated glucagon secretion and altered α-cell function in *Casr*$^{Nuf/Nuf}$ mice. Glucagon plays a central role in systemic glucose homeostasis by stimulating hepatic glucose production, and over-secretion of glucagon contributes to the hyperglycemia in type 2 diabetes (48). The release of glucagon from α-cells is physiologically inhibited by elevations in glucose concentrations (26,48). However, high glucose concentrations failed to suppress glucagon secretion from *Casr*$^{Nuf/Nuf}$ islets. We investigated whether alterations in the electrical activity of *Casr*$^{Nuf/Nuf}$ α-cells may have impaired the suppression of glucagon secretion following exposure to high glucose. In WT α-cells, glucose regulates glucagon secretion via closure of the K_{ATP} channel, and the resulting membrane depolarization leads to reduced activation of P/Q-type VDCCs that mediate the Ca^{2+} entry responsible for hypoglycemia-induced glucagon secretion (26,37,48). However, in *Casr*$^{Nuf/Nuf}$ α-cells, glucose did not induce membrane depolarization, and tolbutamide only caused a modest depolarization (~2mV), whereas this K_{ATP} channel blocker increased membrane potential by ~10 mV in *Casr*$^{+/+}$ α-cells (Figure 9). Together, these data suggest that CaSR activation may have attenuated α-cell basal K_{ATP} channel activity, which impaired the membrane depolarizing effect of glucose and tolbutamide. Furthermore, *Casr*$^{Nuf/Nuf}$ mice exhibited an increase in α-cell numbers within individual islets, enhanced α-cell proliferation rates, and significantly elevated islet glucagon content. These findings highlight a potential and novel role for the CaSR in promoting α-cell neogenesis, but it is also possible that the hypoinsulinemia of *Nuf* mice may have led to an expansion of α-cells, as has previously been reported in mice with streptozotocin-induced insulin deficiency (49).

In conclusion, we have demonstrated that *Nuf* mice with a germline gain-of-function CaSR mutation have impaired glucose tolerance, which can be ameliorated by calcilytic treatment. Moreover, our findings reveal a role for the CaSR in the regulation of pancreatic islet mass, and α- and β-cell function.

References

1. Ashcroft FM, Rorsman P. Diabetes mellitus and the beta cell: the last ten years. Cell 2012; 148:1160-1171

2. Unger RH, Orci L. Paracrinology of islets and the paracrinopathy of diabetes. Proc Natl Acad Sci U S A 2010; 107:16009-16012

3. Stevens RC, Cherezov V, Katritch V, Abagyan R, Kuhn P, Rosen H, Wuthrich K. The GPCR Network: a large-scale collaboration to determine human GPCR structure and function. Nat Rev Drug Discov 2013; 12:25-34

4. Ahren B. Islet G protein-coupled receptors as potential targets for treatment of type 2 diabetes. Nat Rev Drug Discov 2009; 8:369-385

5. Regard JB, Kataoka H, Cano DA, Camerer E, Yin L, Zheng YW, Scanlan TS, Hebrok M, Coughlin SR. Probing cell type-specific functions of Gi in vivo identifies GPCR regulators of insulin secretion. J Clin Invest 2007; 117:4034-4043

6. Hofer AM, Brown EM. Extracellular calcium sensing and signalling. Nat Rev Mol Cell Biol 2003; 4:530-538

7. Regard JB, Sato IT, Coughlin SR. Anatomical profiling of G protein-coupled receptor expression. Cell 2008; 135:561-571

8. Squires PE, Harris TE, Persaud SJ, Curtis SB, Buchan AM, Jones PM. The extracellular calcium-sensing receptor on human beta-cells negatively modulates insulin secretion. Diabetes 2000; 49:409-417

9. Gray E, Muller D, Squires PE, Asare-Anane H, Huang GC, Amiel S, Persaud SJ, Jones PM. Activation of the extracellular calcium-sensing receptor initiates insulin secretion from human islets of Langerhans: involvement of protein kinases. J Endocrinol 2006; 190:703-710

10. Straub SG, Kornreich B, Oswald RE, Nemeth EF, Sharp GW. The calcimimetic R-467 potentiates insulin secretion in pancreatic beta cells by activation of a nonspecific cation channel. J Biol Chem 2000; 275:18777-18784

11. Oh YS, Seo EH, Lee YS, Cho SC, Jung HS, Park SC, Jun HS. Increase of Calcium Sensing Receptor Expression Is Related to Compensatory Insulin Secretion during Aging in Mice. PLoS One 2016; 11:e0159689

12. Babinsky VN, Hannan FM, Youhanna SC, Marechal C, Jadoul M, Devuyst O, Thakker RV. Association studies of calcium-sensing receptor (CaSR) polymorphisms with serum concentrations of glucose and phosphate, and vascular calcification in renal transplant recipients. PLoS One 2015; 10:e0119459

13. Wolf P, Krssak M, Winhofer Y, Anderwald CH, Zwettler E, Just Kukurova I, Gessl A, Trattnig S, Luger A, Baumgartner-Parzer S, Krebs M. Cardiometabolic phenotyping of patients with familial hypocalcuric hypercalcemia. J Clin Endocrinol Metab 2014; 99:E1721-1726

14. Hannan FM, Babinsky VN, Thakker RV. Disorders of the calcium-sensing receptor and partner proteins: insights into the molecular basis of calcium homeostasis. J Mol Endocrinol 2016; 57:R127-142

15. Hannan FM, Walls GV, Babinsky VN, Nesbit MA, Kallay E, Hough TA, Fraser WD, Cox RD, Hu J, Spiegel AM, Thakker RV. The Calcilytic Agent NPS 2143 Rectifies Hypocalcemia in a Mouse Model With an Activating Calcium-Sensing Receptor (CaSR) Mutation: Relevance to Autosomal Dominant Hypocalcemia Type 1 (ADH1). Endocrinology 2015; 156:3114-3121

16. Hough TA, Bogani D, Cheeseman MT, Favor J, Nesbit MA, Thakker RV, Lyon MF. Activating calcium-sensing receptor mutation in the mouse is associated with cataracts and ectopic calcification. Proc Natl Acad Sci U S A 2004; 101:13566-13571

17. Hannan FM, Howles SA, Rogers A, Cranston T, Gorvin CM, Babinsky VN, Reed AA, Thakker CE, Bockenhauer D, Brown RS, Connell JM, Cook J, Darzy K, Ehtisham S, Graham U, Hulse T, Hunter SJ, Izatt L, Kumar D, McKenna MJ, McKnight JA, Morrison PJ, Mughal MZ, O'Halloran D, Pearce SH, Porteous ME, Rahman M, Richardson T, Robinson R, Scheers I, Siddique H, Van't Hoff WG, Wang T, Whyte MP, Nesbit MA, Thakker RV. Adaptor protein-2 sigma subunit mutations causing familial hypocalciuric hypercalcaemia type 3

(FHH3) demonstrate genotype-phenotype correlations, codon bias and dominant-negative effects. Hum Mol Genet 2015; 24:5079-5092

18. Babinsky VN, Hannan FM, Gorvin CM, Howles SA, Nesbit MA, Rust N, Hanyaloglu AC, Hu J, Spiegel AM, Thakker RV. Allosteric Modulation of the Calcium-Sensing Receptor Rectifies Signaling Abnormalities Associated with G-protein alpha-11 Mutations causing Hypercalcemic and Hypocalcemic Disorders. J Biol Chem 2016; 291:10876-10885

19. Goldsworthy M, Hugill A, Freeman H, Horner E, Shimomura K, Bogani D, Pieles G, Mijat V, Arkell R, Bhattacharya S, Ashcroft FM, Cox RD. Role of the transcription factor sox4 in insulin secretion and impaired glucose tolerance. Diabetes 2008; 57:2234-2244

20. Prior RL, Wu X, Gu L, Hager TJ, Hager A, Howard LR. Whole berries versus berry anthocyanins: interactions with dietary fat levels in the C57BL/6J mouse model of obesity. J Agric Food Chem 2008; 56:647-653

21. Zhang Q, Chibalina MV, Bengtsson M, Groschner LN, Ramracheya R, Rorsman NJ, Leiss V, Nassar MA, Welling A, Gribble FM, Reimann F, Hofmann F, Wood JN, Ashcroft FM, Rorsman P. Na+ current properties in islet alpha- and beta-cells reflect cell-specific Scn3a and Scn9a expression. J Physiol 2014; 592:4677-4696

22. Hobaus J, Hummel DM, Thiem U, Fetahu IS, Aggarwal A, Mullauer L, Heller G, Egger G, Mesteri I, Baumgartner-Parzer S, Kallay E. Increased copy-number and not DNA hypomethylation causes overexpression of the candidate proto-oncogene CYP24A1 in colorectal cancer. Int J Cancer 2013; 133:1380-1388

23. Bentley L, Esapa CT, Nesbit MA, Head RA, Evans H, Lath D, Scudamore CL, Hough TA, Podrini C, Hannan FM, Fraser WD, Croucher PI, Brown MA, Brown SD, Cox RD, Thakker RV. An N-ethyl-N-nitrosourea induced corticotropin-releasing hormone promoter mutation provides a mouse model for endogenous glucocorticoid excess. Endocrinology 2014; 155:908-922

24. De Marinis YZ, Salehi A, Ward CE, Zhang Q, Abdulkader F, Bengtsson M, Braha O, Braun M, Ramracheya R, Amisten S, Habib AM, Moritoh Y, Zhang E, Reimann F, Rosengren AH, Shibasaki T, Gribble F, Renstrom E, Seino S, Eliasson L, Rorsman P. GLP-1 inhibits and adrenaline stimulates glucagon release by differential modulation of N- and L-type Ca2+ channel-dependent exocytosis. Cell Metab 2010; 11:543-553

25. Shigeto M, Ramracheya R, Tarasov AI, Cha CY, Chibalina MV, Hastoy B, Philippaert K, Reinbothe T, Rorsman N, Salehi A, Sones WR, Vergari E, Weston C, Gorelik J, Katsura M, Nikolaev VO, Vennekens R, Zaccolo M, Galione A, Johnson PR, Kaku K, Ladds G, Rorsman P. GLP-1 stimulates insulin secretion by PKC-dependent TRPM4 and TRPM5 activation. J Clin Invest 2015; 125:4714-4728

26. Rorsman P, Ramracheya R, Rorsman NJ, Zhang Q. ATP-regulated potassium channels and voltage-gated calcium channels in pancreatic alpha and beta cells: similar functions but reciprocal effects on secretion. Diabetologia 2014; 57:1749-1761

27. Aggarwal A, Prinz-Wohlgenannt M, Groschel C, Tennakoon S, Meshcheryakova A, Chang W, Brown EM, Mechtcheriakova D, Kallay E. The calcium-sensing receptor suppresses epithelial-to-mesenchymal transition and stem cell- like phenotype in the colon. Molecular cancer 2015; 14:61

28. de Winter JC. Using the Student's t-test with extremely small sample sizes. Practical Assessment, Research & Evaluation 2013; 18

29. Fitzpatrick LA, Dabrowski CE, Cicconetti G, Gordon DN, Papapoulos S, Bone HG, 3rd, Bilezikian JP. The effects of ronacaleret, a calcium-sensing receptor antagonist, on bone mineral density and biochemical markers of bone turnover in postmenopausal women with low bone mineral density. J Clin Endocrinol Metab 2011; 96:2441-2449

30. Medina J, Nakagawa Y, Nagasawa M, Fernandez A, Sakaguchi K, Kitaguchi T, Kojima I. Positive Allosteric Modulation of the Calcium-sensing Receptor by Physiological Concentrations of Glucose. J Biol Chem 2016; 291:23126-23135

31. Golson ML, Dunn JC, Maulis MF, Dadi PK, Osipovich AB, Magnuson MA, Jacobson DA, Gannon M. Activation of FoxM1 Revitalizes the Replicative Potential of Aged beta-Cells in Male Mice and Enhances Insulin Secretion. Diabetes 2015; 64:3829-3838

32. Kitamura T, Nakae J, Kitamura Y, Kido Y, Biggs WH, 3rd, Wright CV, White MF, Arden KC, Accili D. The forkhead transcription factor Foxo1 links insulin signaling to Pdx1 regulation of pancreatic beta cell growth. J Clin Invest 2002; 110:1839-1847

33. Takamoto I, Kubota N, Nakaya K, Kumagai K, Hashimoto S, Kubota T, Inoue M, Kajiwara E, Katsuyama H, Obata A, Sakurai Y, Iwamoto M, Kitamura T, Ueki K, Kadowaki T. TCF7L2 in mouse pancreatic beta cells plays a crucial role in glucose homeostasis by regulating beta cell mass. Diabetologia 2014; 57:542-553

34. Xu X, D'Hoker J, Stange G, Bonne S, De Leu N, Xiao X, Van de Casteele M, Mellitzer G, Ling Z, Pipeleers D, Bouwens L, Scharfmann R, Gradwohl G, Heimberg H. Beta cells can be generated from endogenous progenitors in injured adult mouse pancreas. Cell 2008; 132:197-207

35. Gage BK, Asadi A, Baker RK, Webber TD, Wang R, Itoh M, Hayashi M, Miyata R, Akashi T, Kieffer TJ. The Role of ARX in Human Pancreatic Endocrine Specification. PLoS One 2015; 10:e0144100

36. MacConaill M. Calcium precipitation from mammalian physiological salines (Ringer solutions) and the preparation of high [Ca] media. J Pharmacol Methods 1985; 14:147-155

37. Zhang Q, Ramracheya R, Lahmann C, Tarasov A, Bengtsson M, Braha O, Braun M, Brereton M, Collins S, Galvanovskis J, Gonzalez A, Groschner LN, Rorsman NJ, Salehi A, Travers ME, Walker JN, Gloyn AL, Gribble F, Johnson PR, Reimann F, Ashcroft FM, Rorsman P. Role of KATP channels in glucose-regulated glucagon secretion and impaired counterregulation in type 2 diabetes. Cell Metab 2013; 18:871-882

38. Nemeth EF, Goodman WG. Calcimimetic and Calcilytic Drugs: Feats, Flops, and Futures. Calcif Tissue Int 2016; 98:341-358

39. Yasuda K, Hurukawa Y, Okuyama M, Kikuchi M, Yoshinaga K. Glucose tolerance and insulin secretion in patients with parathyroid disorders. Effect of serum calcium on insulin release. N Engl J Med 1975; 292:501-504

40. Bravo-Sagua R, Mattar P, Diaz X, Lavandero S, Cifuentes M. Calcium Sensing Receptor as a Novel Mediator of Adipose Tissue Dysfunction: Mechanisms and Potential Clinical Implications. Front Physiol 2016; 7:395

41. Xie J, Jiang Y, Kan Y, Zhao J, Kuang H, Ge P. Calcium-sensing receptor is involved in the pathogenesis of fat emulsion-induced insulin resistance in rats. Mol Med Rep 2015; 12:2043-2048

42. Berger M, Scheel DW, Macias H, Miyatsuka T, Kim H, Hoang P, Ku GM, Honig G, Liou A, Tang Y, Regard JB, Sharifnia P, Yu L, Wang J, Coughlin SR, Conklin BR, Deneris ES, Tecott LH, German MS. Galphai/o-coupled receptor signaling restricts pancreatic beta-cell expansion. Proc Natl Acad Sci U S A 2015; 112:2888-2893

43. Walls GV, Reed AA, Jeyabalan J, Javid M, Hill NR, Harding B, Thakker RV. Proliferation rates of multiple endocrine neoplasia type 1 (MEN1)-associated tumors. Endocrinology 2012; 153:5167-5179

44. Butler AE, Janson J, Bonner-Weir S, Ritzel R, Rizza RA, Butler PC. Beta-cell deficit and increased beta-cell apoptosis in humans with type 2 diabetes. Diabetes 2003; 52:102-110

45. Ashcroft FM, Rorsman P. K(ATP) channels and islet hormone secretion: new insights and controversies. Nat Rev Endocrinol 2013; 9:660-669

46. Braun M, Ramracheya R, Bengtsson M, Zhang Q, Karanauskaite J, Partridge C, Johnson PR, Rorsman P. Voltage-gated ion channels in human pancreatic beta-cells: electrophysiological characterization and role in insulin secretion. Diabetes 2008; 57:1618-1628

47. Parkash J. Glucose-mediated spatial interactions of voltage dependent calcium channels and calcium sensing receptor in insulin producing beta-cells. Life sciences 2011; 88:257-264

48. Briant L, Salehi A, Vergari E, Zhang Q, Rorsman P. Glucagon secretion from pancreatic alpha-cells. Ups J Med Sci 2016; 121:113-119

49. Li Z, Karlsson FA, Sandler S. Islet loss and alpha cell expansion in type 1 diabetes induced by multiple low-dose streptozotocin administration in mice. J Endocrinol 2000; 165:93-99

Figure legends

Figure 1. Plasma glucose, insulin and glucagon concentrations during intraperitoneal glucose tolerance (IPGTT) testing. (A) Male and (B) female *Casr*$^{Nuf/+}$ (blue) and *Casr*$^{Nuf/Nuf}$ mice (red) are significantly hyperglycemic compared to respective Casr$^{+/+}$ mice (black) during a 2 hour IPGTT. (C) Male and (D) female *Casr*$^{Nuf/Nuf}$ mice, and male *Casr*$^{Nuf/+}$ mice have significantly reduced plasma insulin concentrations compared to respective *Casr*$^{+/+}$ mice during a 30 min IPGTT. (E) Male and (F) female *Casr*$^{Nuf/Nuf}$ mice show significant elevations in plasma glucagon concentrations compared to respective *Casr*$^{+/+}$ mice during a 2 hour IPGTT. Results are expressed as mean ± SEM. *$p < 0.05$, **$p < 0.01$, ***$p < 0.001$ compared to *Casr*$^{+/+}$ mice at respective time-points.

Figure 2. Effect of ronacaleret on the CaSR gain-of-function and hypocalcemia of *Nuf* mice. (A) Fluorescence microscopy of HEK293 cells transiently transfected with WT Leu723 or mutant (m) Gln723 CASR-pEGFP-N1 constructs. GFP expression in these cells indicates successful transfection and expression by these constructs. Bar indicates 10 μm. (B) Effect of ronacaleret treatment on the intracellular calcium responses of the Gln723 CaSR mutant. The Gln723 CaSR mutant led to a leftward shift in the concentration-response curve (solid red line) compared to the WT (Leu723) CaSR (solid black line). The addition of ronacaleret (Rona) at 20 nM and 40 nM concentrations rectified the leftward shift of the Gln723 CaSR mutant (red dotted line and red dashed line, respectively). The zoomed-in image shows the concentration-response curves at the EC_{50} values of the WT and mutant CaSRs. (C) Effect of 20 nM and 40 nM ronacaleret on the EC_{50} values of the Gln723 CaSR mutant. (D) Male and (E) female *Casr*$^{Nuf/+}$ and *Casr*$^{Nuf/Nuf}$ mice were significantly hypocalcemic compared to respective *Casr*$^{+/+}$ mice. Treatment with 90 mg/kg ronacaleret significantly increased plasma calcium concentrations in Casr$^{+/+}$, *Casr*$^{Nuf/+}$ and *Casr*$^{Nuf/Nuf}$ mice compared to respective mice treated with the drug vehicle only. Ronacaleret treatment normalised the plasma calcium concentrations of *Casr*$^{Nuf/+}$ mice. However, the plasma calcium concentrations of treated *Casr*$^{Nuf/Nuf}$ mice remained significantly reduced compared to untreated *Casr*$^{+/+}$ mice. Mean ± SEM values are indicated by solid bars. NS, non-significant, *$p < 0.05$, **$p < 0.01$, ***$p < 0.001$.

Figure 3. Effect of ronacaleret on the plasma glucose, insulin and glucagon concentrations of male mice during intraperitoneal glucose tolerance testing (IPGTT). Ronacaleret administration had no effect on the plasma glucose concentrations of (A) *Casr*$^{+/+}$ mice (black dashed line), but significantly lowered plasma glucose in (B) *Casr*$^{Nuf/+}$ (blue dashed line) and (C) *Casr*$^{Nuf/Nuf}$ mice (red dashed line) compared to respective control mice treated with the drug vehicle only (represented by solid lines), so that the glucose concentrations were not significantly different from *Casr*$^{+/+}$ mice. Ronacaleret had no effect on the plasma insulin concentrations of (D) *Casr*$^{+/+}$ mice, but significantly increased plasma insulin in (E) *Casr*$^{Nuf/+}$ mice compared to controls, so that the insulin concentrations were not significantly different from *Casr*$^{+/+}$ mice. Ronacaleret treatment did not alter plasma insulin concentrations in (F) *Casr*$^{Nuf/Nuf}$ mice. Ronacaleret had no significant effect on the plasma glucagon concentrations of (G) *Casr*$^{+/+}$ mice, (H) *Casr*$^{Nuf/+}$ mice, or (I) *Casr*$^{Nuf/Nuf}$ mice compared to respective control mice. Results are expressed as mean ± SEM. *$p < 0.05$, **$p < 0.01$ compared to control mice.

Figure 4. Effect of ronacaleret on the plasma glucose, insulin and glucagon concentrations of female mice during intraperitoneal glucose tolerance testing (IPGTT). Ronacaleret administration had no effect on the plasma glucose concentrations of (A) *Casr*$^{+/+}$ mice (black dashed line), but significantly lowered plasma glucose in (B) *Casr*$^{Nuf/+}$ (blue dashed line) and (C) *Casr*$^{Nuf/Nuf}$ mice (red dashed line) compared to respective control mice treated with the drug vehicle only (represented by solid lines), so that the glucose concentrations were not significantly different from *Casr*$^{+/+}$ mice. Ronacaleret had no effect on the plasma insulin concentrations of (D) *Casr*$^{+/+}$ mice, but significantly increased plasma insulin in (E) *Casr*$^{Nuf/+}$ mice compared to controls, so that the insulin concentrations were not significantly different from *Casr*$^{+/+}$ mice. Ronacaleret treatment did not alter plasma insulin concentrations in (F) *Casr*$^{Nuf/Nuf}$ mice. Ronacaleret had no significant effect on the plasma glucagon concentrations of (G) *Casr*$^{+/+}$ mice, (H) *Casr*$^{Nuf/+}$ mice, or (I) *Casr*$^{Nuf/Nuf}$ mice compared to respective control mice. Results are expressed as mean ± SEM. *$p < 0.05$, **$p < 0.01$, ***$p < 0.001$ compared to control mice.

Figure 5. Histological analysis of *Nuf* mice pancreatic islets. (A) Representative H&E stained pancreatic sections from *Casr*$^{+/+}$, *Casr*$^{Nuf/+}$ and *Casr*$^{Nuf/Nuf}$ mice. Bars indicate 200µm. (B) Islet area and (C) number are significantly reduced in *Casr*$^{Nuf/+}$ and *Casr*$^{Nuf/Nuf}$ mice compared to *Casr*$^{+/+}$ mice. (D) Islet size is significantly reduced in *Casr*$^{Nuf/Nuf}$ mice compared to *Casr*$^{+/+}$ mice. (E) Representative pancreatic islets from *Casr*$^{+/+}$, *Casr*$^{Nuf/+}$ and *Casr*$^{Nuf/Nuf}$ mice immunostained for glucagon (red), insulin (white) and DAPI (blue). Bars indicate 50µm. (F) *Casr*$^{Nuf/Nuf}$ mice have significantly reduced β-cell numbers and (G) significantly increased α-cell numbers compared to *Casr*$^{+/+}$ mice. (H) β-cell proliferation in representative islets from *Casr*$^{+/+}$, *Casr*$^{Nuf/+}$ and *Casr*$^{Nuf/Nuf}$ mice immunostained for insulin (white), DAPI (blue) and KI-67 (red). KI-67 positive cells are also indicated by yellow arrows. Bars indicate 50µm. (I) *Casr*$^{Nuf/Nuf}$ mice have significantly reduced proliferation of β-cells and (J) significantly increased proliferation of α-cells compared to respective *Casr*$^{+/+}$ mice. Results are expressed as mean ± SEM. *$p < 0.05$, **$p < 0.01$ compared to *Casr*$^{+/+}$ mice.

Figure 6. Insulin and glucagon secretion from isolated *Nuf* mice pancreatic islets. (A) The total insulin content of *Casr*$^{Nuf/Nuf}$ islets was not altered compared to *Casr*$^{+/+}$ islets. (B) *Casr*$^{+/+}$ and *Casr*$^{Nuf/Nuf}$ islets were incubated in 1.6 mM $[Ca^{2+}]_o$ and exposed to varying glucose concentrations (1 mM, 6 mM or 20 mM). *Casr*$^{+/+}$ and *Casr*$^{Nuf/Nuf}$ islets showed significantly increased insulin secretion following stimulation with 20 mM glucose. No significant differences in the maximal insulin secretory responses were observed between *Casr*$^{+/+}$ and *Casr*$^{Nuf/Nuf}$ islets. (C) The total glucagon content of *Casr*$^{Nuf/Nuf}$ islets was significantly increased compared to *Casr*$^{+/+}$ islets. (D) *Casr*$^{+/+}$ and *Casr*$^{Nuf/Nuf}$ islets were incubated in 1.6 mM $[Ca^{2+}]_o$ and exposed to 1 mM and 6 mM glucose concentrations. *Casr*$^{+/+}$ islets showed a significant reduction in glucagon secretion following stimulation with 6 mM glucose. In contrast, glucagon secretion from *Casr*$^{Nuf/Nuf}$ islets failed to suppress following glucose stimulation, and *Casr*$^{Nuf/Nuf}$ islets had significantly increased glucagon secretion compared to *Casr*$^{+/+}$ islets at 6 mM glucose. (E) The effect of extracellular calcium (Ca^{2+}_o) on insulin secretion was assessed by incubating *Casr*$^{+/+}$ and *Casr*$^{Nuf/Nuf}$ islets with varying Ca^{2+}_o concentrations (0.8 mM or 1.6 mM) and exposing them to low (1 mM) or high (20 mM) glucose. Exposure to low (0.8 mM) Ca^{2+}_o suppressed insulin secretion from *Casr*$^{+/+}$ and *Casr*$^{Nuf/Nuf}$ islets at 20 mM glucose. (F) Exposure to low

(0.8 mM) Ca^{2+}_o increased glucagon secretion from *Casr*$^{+/+}$ islets at 20 mM glucose, but had no effect on glucagon secretion from *Casr*$^{Nuf/Nuf}$ islets. Islet insulin and glucagon in A-D was measured by radioimmunoassay, and by duplex Rat/Mouse ELISA (Meso Scale Discovery) in E-F. The sample size (N) represents batches of size-matched islets, which were pooled from 3-6 *Casr*$^{+/+}$ mice and 6 *Casr*$^{Nuf/Nuf}$ mice. Mean ± SEM values for the respective groups are indicated by solid bars. NS, non-significant, *p < 0.05, **p <0.01, ***p < 0.001.

Figure 7. Effect of glucose stimulation on the electrical activity of *Nuf* mice β-cells. (A) Representative membrane potential recording of β-cells from intact *Casr*$^{+/+}$ and *Casr*$^{Nuf/Nuf}$ after islets had been incubated in 1.5 mM $[Ca^{2+}]_o$ and following stimulation with 1 mM (1G), 12 mM (12G) and 20 mM (20G) glucose concentrations or with tolbutamide (Tolb). (B) Representative membrane potential recording of β-cells from intact *Casr*$^{+/+}$ and *Casr*$^{Nuf/Nuf}$ islets in the presence of 0.75 mM Ca^{2+}_o concentrations and following stimulation with 1, 12, or 20 mM glucose concentrations or with tolbutamide. (C) Basal membrane potential, (D) action potential peak, (E) anti-peak potential, and (F) frequency of action potential firing from β-cells was assessed in intact *Casr*$^{+/+}$ (open bars) and *Casr*$^{Nuf/Nuf}$ islets (black bars) in the presence of 1.5 or 0.75 mM Ca^{2+}_o concentrations and following stimulation with glucose or tolbutamide. The sample size (N) represents individual β-cell recordings obtained from intact islets of 6 *Casr*$^{+/+}$ mice and 4 *Casr*$^{Nuf/Nuf}$ mice. Results are expressed as mean ± SEM. *p <0.05, **p <0.01 compared to *Casr*$^{+/+}$ mice at respective glucose and Ca^{2+}_o concentrations.

Figure 8. K_{ATP} channel conductance of *Nuf* mice β-cells. (A) Representative recording of β-cell K_{ATP} channel conductance from intact *Casr*$^{+/+}$ and *Casr*$^{Nuf/Nuf}$ islets after islets had been incubated in 1.5 mM $[Ca^{2+}]_o$ and following stimulation with 1 mM (1G), 12 mM (12G) and 20 mM (20G) glucose concentrations or with tolbutamide (Tolb). (B) Analysis of K_{ATP} channel conductance from β-cells within intact *Casr*$^{+/+}$ (open bars) and *Casr*$^{Nuf/Nuf}$ islets (black bars) following stimulation with glucose or tolbutamide. (C) Representative traces of β-cell background current measurement following glucose stimulation or treatment with tolbutamide. (D) Analysis of holding current from β-cells within intact *Casr*$^{+/+}$ (open bars) and *Casr*$^{Nuf/Nuf}$ islets (black bars) following stimulation with glucose or

tolbutamide. The sample size (N) represents individual β-cell recordings obtained from intact islets of 5 *Casr*$^{+/+}$ mice and 5 *Casr*$^{Nuf/Nuf}$ mice. Results are expressed as mean ± SEM. *p < 0.05, **p < 0.01 compared to *Casr*$^{+/+}$ mice at respective glucose and tolbutamide concentrations.

Figure 9. Effect of glucose stimulation on the electrical activity of *Nuf* mice α-cells. Representative membrane potential recording of α-cells from (A) intact *Casr*$^{+/+}$ and (B) *Casr*$^{Nuf/Nuf}$ islets after islets had been incubated in 1.5 mM $[Ca^{2+}]_o$ and following stimulation with 1 mM (1G) and 6 mM (6G) glucose concentrations or with tolbutamide (Tolb). (C) Anti-peak potential, (D) action potential peak, and (E) frequency of action potential firing was assessed in α-cells within intact *Casr*$^{+/+}$ (open bars) and *Casr*$^{Nuf/Nuf}$ islets (black bars) following stimulation with glucose or tolbutamide. The sample size (N) represents individual α-cell recordings obtained from intact islets of 5 *Casr*$^{+/+}$ mice and 7 *Casr*$^{Nuf/Nuf}$ mice. Results are expressed as mean ± SEM. *p <0.05, **p <0.01 compared to respective α-cells at 1 mM glucose.

Figure 1

Click here to download Figure Figure 1.tif

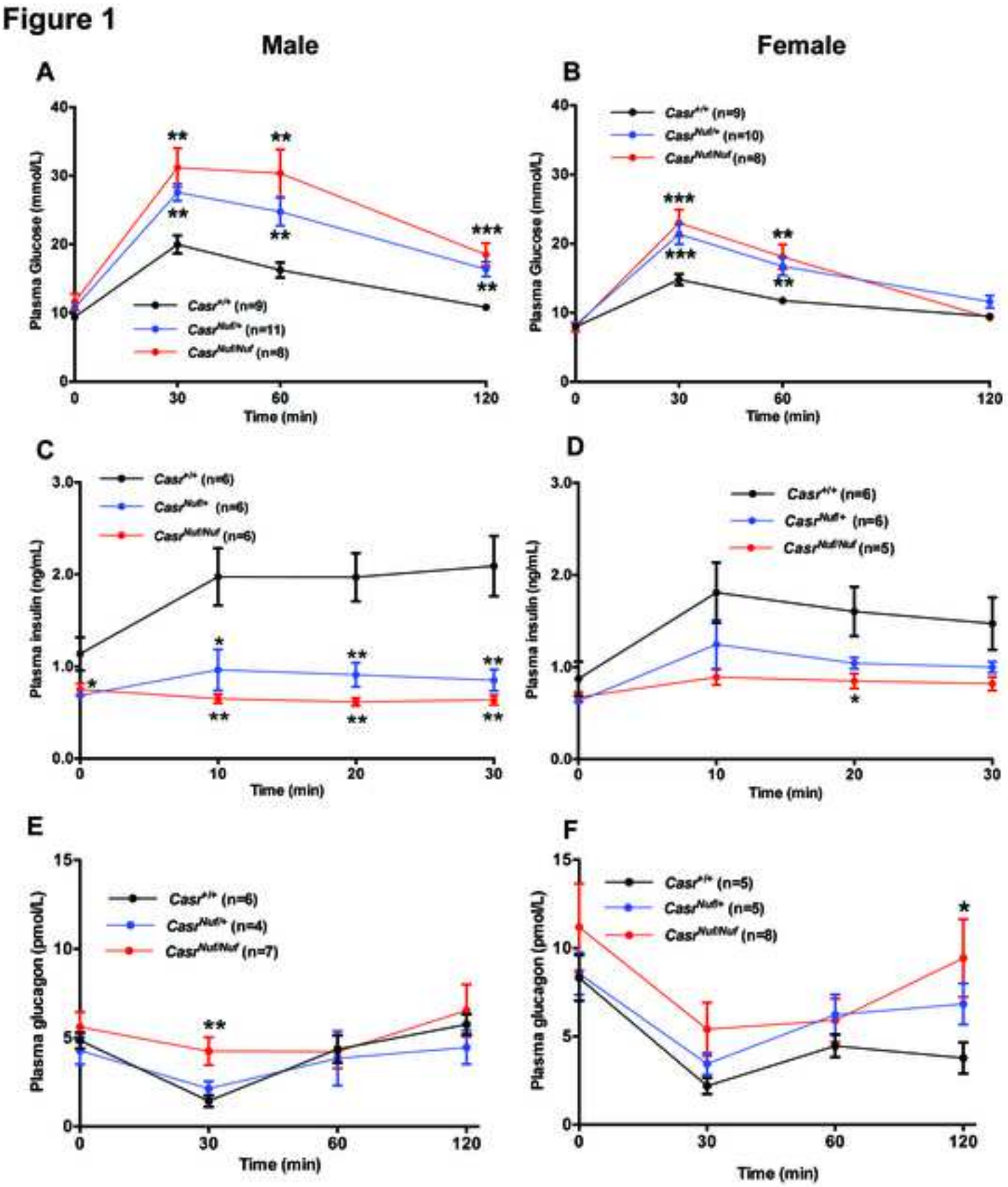

Figure 2

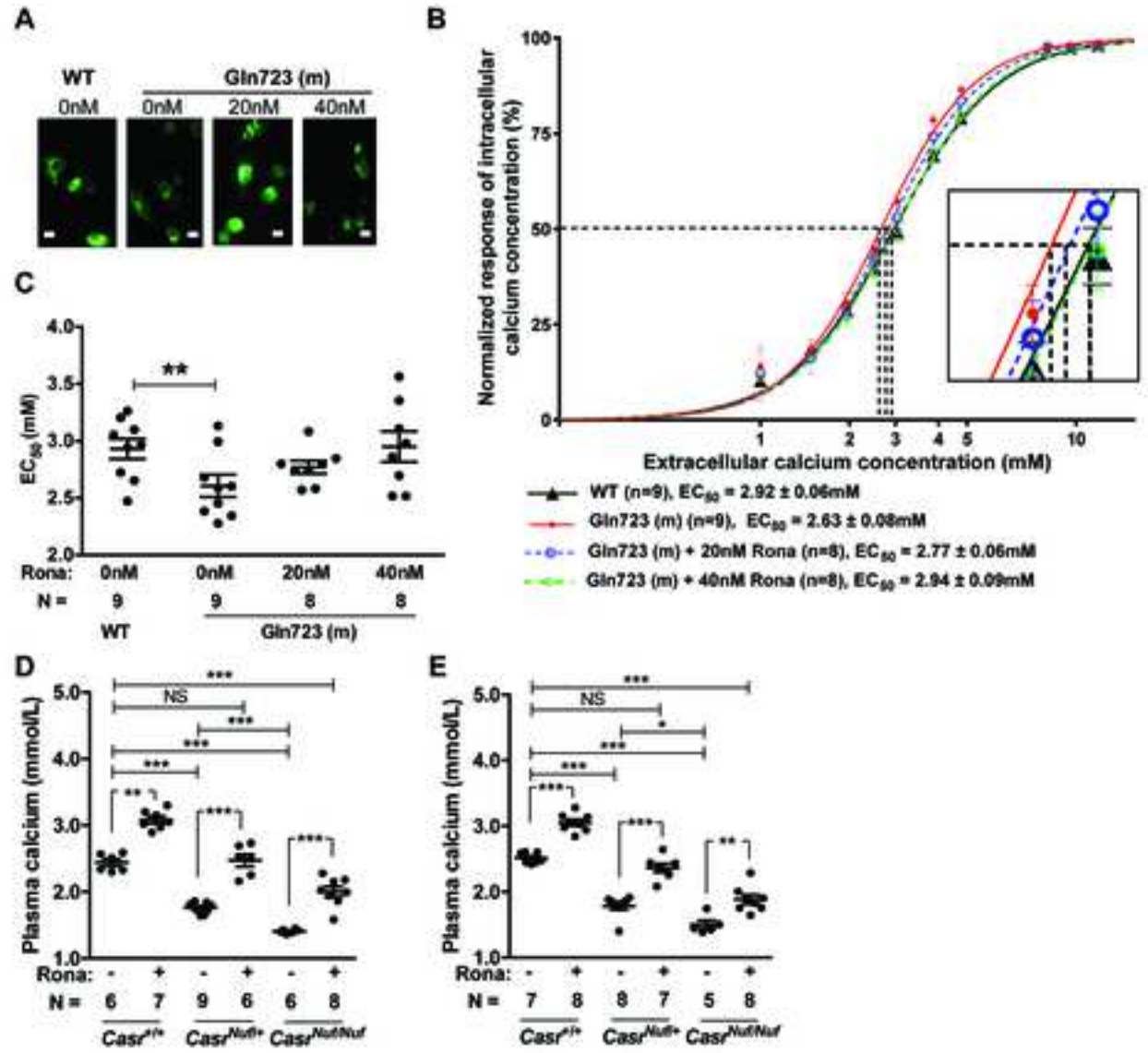
A
WT
Gln723 (m)
0nM
0nM
20nM
40nM
B
Normalized response of intracellular calcium concentration (%)
Extracellular calcium concentration (mM)
WT (n=9), EC50 = 2.92 ± 0.06mM
Gln723 (m) (n=9), EC50 = 2.63 ± 0.08mM
Gln723 (m) + 20nM Rona (n=8), EC50 = 2.77 ± 0.06mM
Gln723 (m) + 40nM Rona (n=8), EC50 = 2.94 ± 0.09mM
C
EC50 (mM)
Rona: 0nM 0nM 20nM 40nM
N = 9 9 8 8
WT
Gln723 (m)
D
Plasma calcium (mmol/L)
NS
Rona: - + - + - +
N = 6 7 9 6 6 8
Casr+/+ CasrNut/+ CasrNut/Nut
E
Plasma calcium (mmol/L)
NS
Rona: - + - + - +
N = 7 8 8 7 5 8
Casr+/+ CasrNut/+ CasrNut/Nut

Figure 3

Click here to download Figure Figure 3.tif

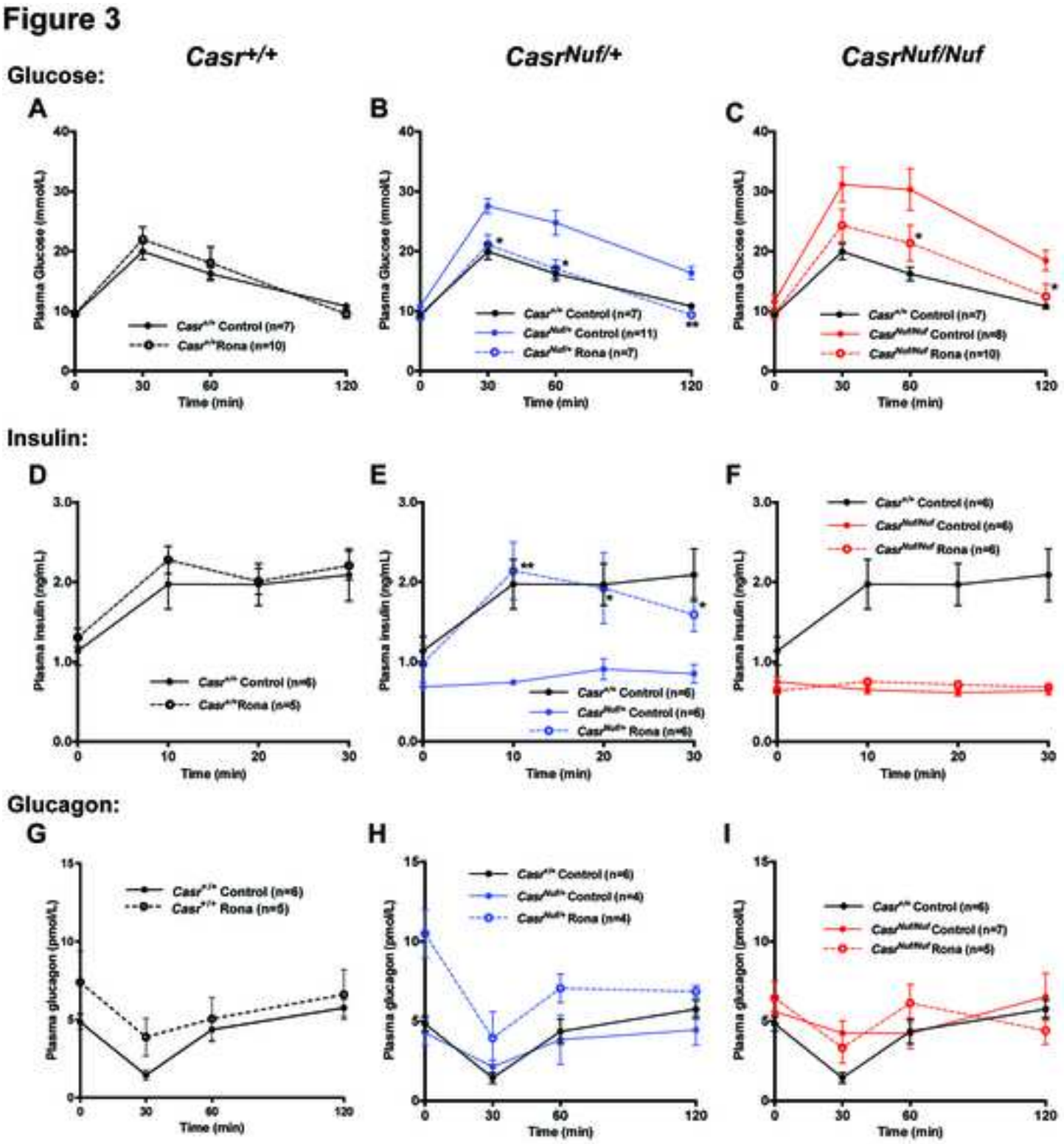

Figure 4

Click here to download Figure Figure 4.tif

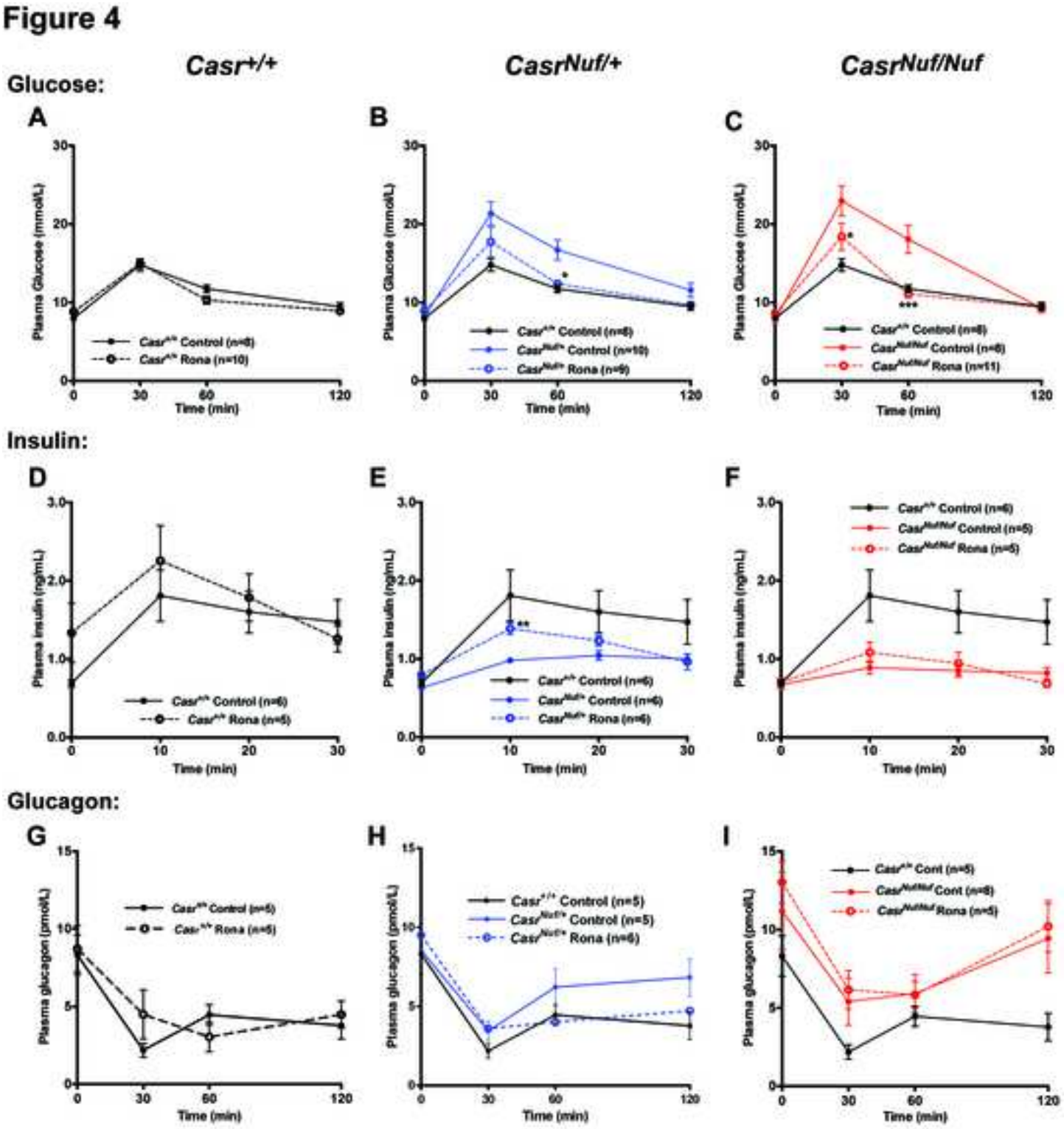

Figure 5

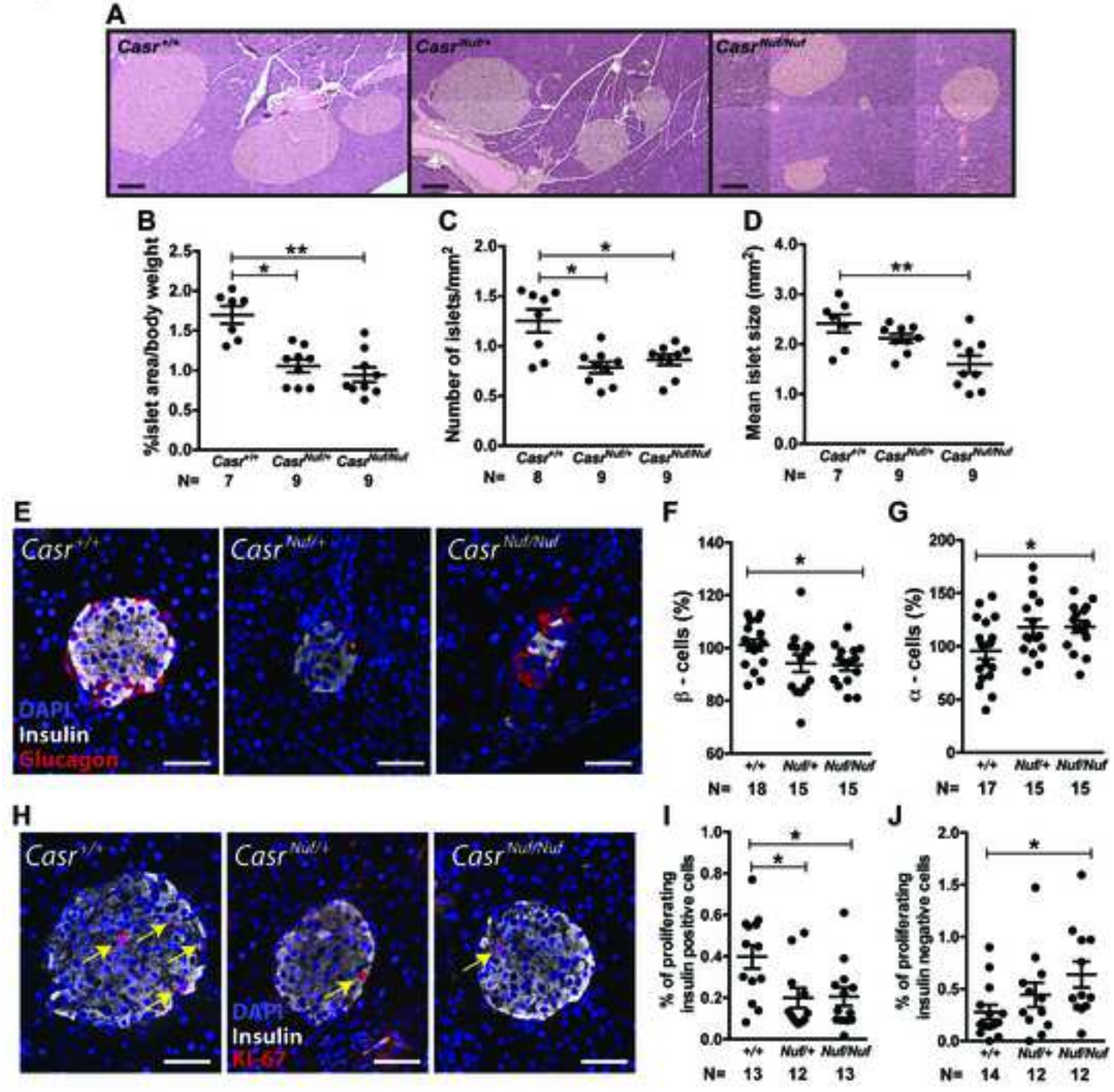

Figure 6

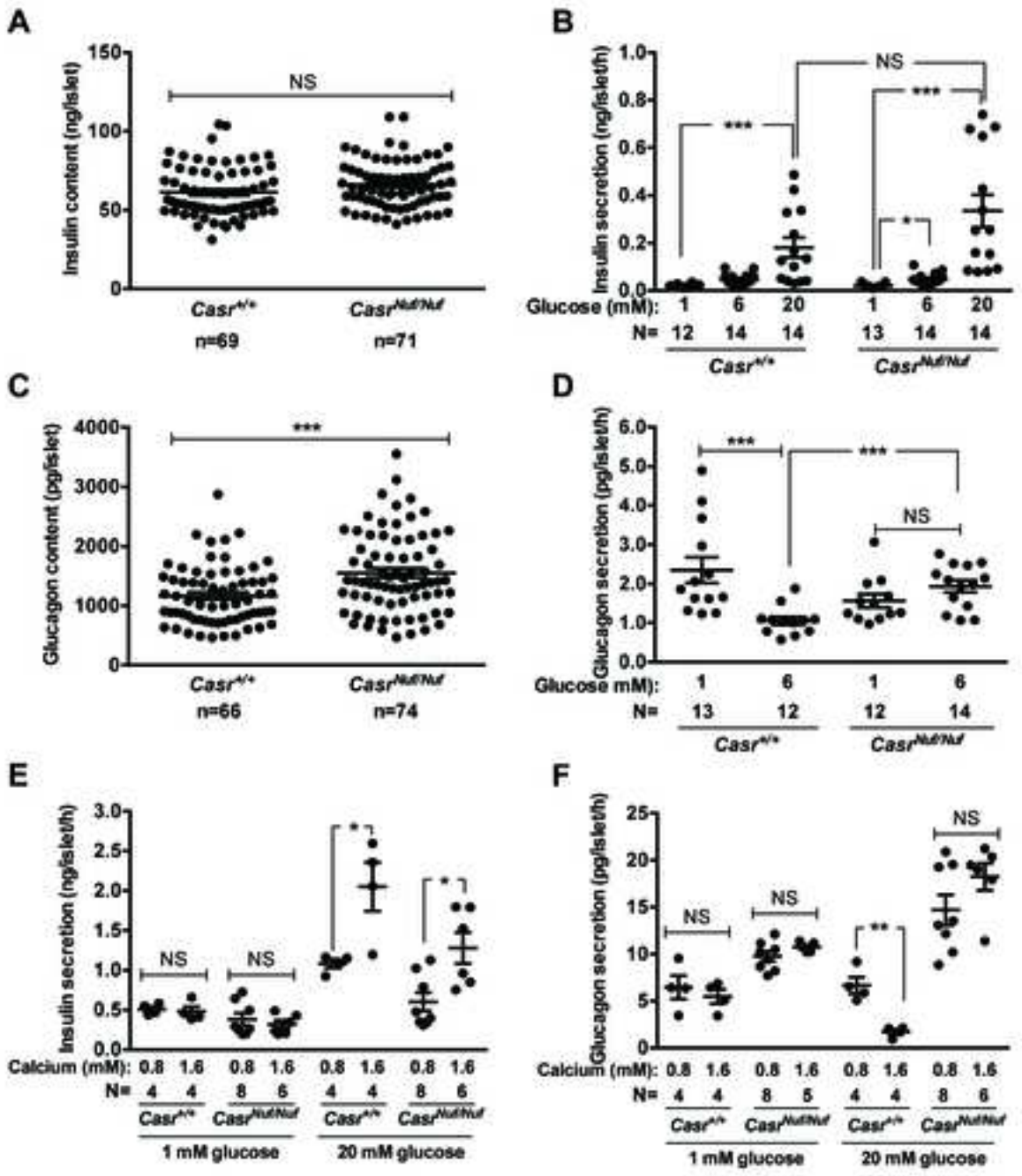

Figure 7

Click here to download Figure Figure 7.tif

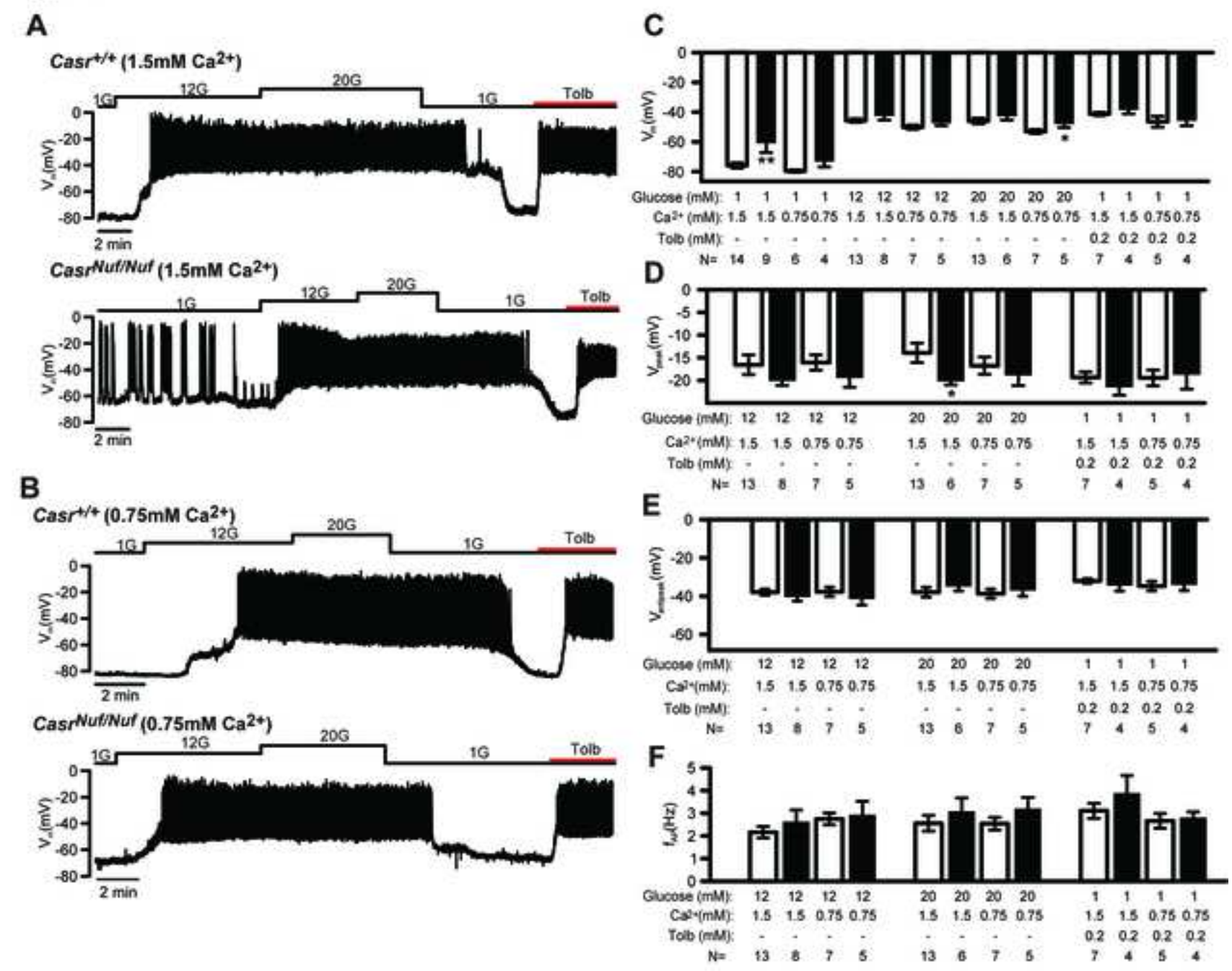

Figure 8

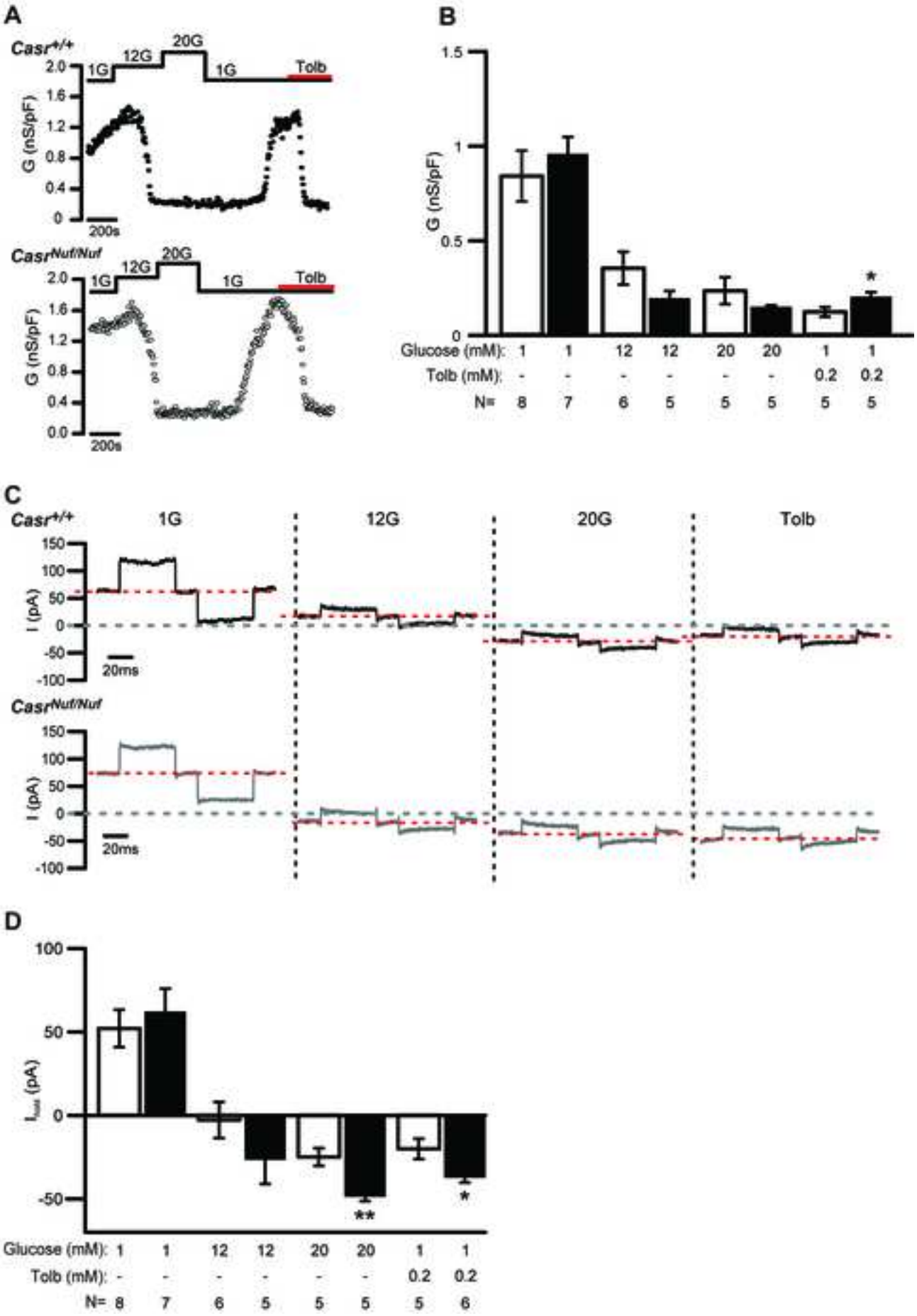

Figure 9

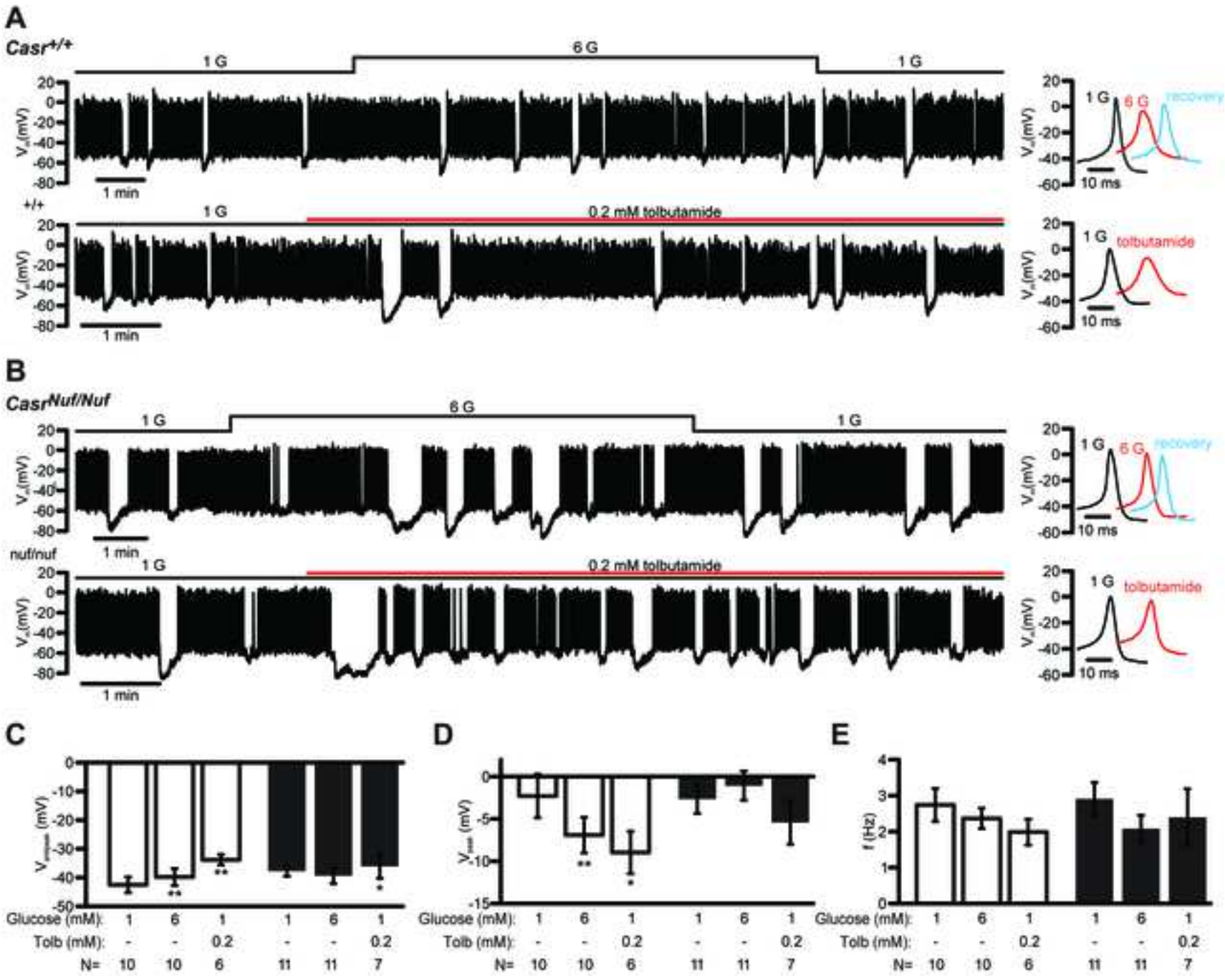

Antibody Table

Peptide/protein target	Antigen sequence (if known)	Name of Antibody	Manufacturer, catalog #, and/or name of individual providing the antibody	Species raised in; monoclonal or polyclonal	Dilution used
Primary antibodies					
Insulin		Anti-insulin	abcam, ab7842	guinea pig; polyclonal	0.005
Glucagon		Anti-glucagon	abcam, ab92517	rabbit; monoclonal	0.005
Ki67		Anti-Ki67	abcam, ab15580	rabbit; polyclonal	0.002
Secondary antibodies					
Anti-Guinea pig IgG (H+L)		Cy™2 AffiniPure Donkey Anti-Guinea Pig IgG (H·	Jackson, 706-225-148	donkey; polyclonal	0.01
Anti-Rabbit IgG (H+L)		Cy™3 AffiniPure Donkey Anti-Rabbit IgG (H+L)	Jackson, 711-165-152	donkey; polyclonal	0.002